HHS Public Access

Author manuscript

Dev Biol. Author manuscript; available in PMC 2018 April 15.

Published in final edited form as:

Dev Biol. 2017 April 15; 424(2): 162–180. doi:10.1016/j.ydbio.2017.03.004.

Satellite-like cells contribute to *pax7*-dependent skeletal muscle repair in adult zebrafish

Michael A. Berberoglu[a,b], **Thomas L. Gallagher**[a,b], **Zachary T. Morrow**[a,b], **Jared C. Talbot**[a,b], **Kimberly J. Hromowyk**[a,b], **Inês M. Tenente**[c], **David M. Langenau**[c], and **Sharon L. Amacher**[a,b,*]

[a]Departments of Molecular Genetics and Biological Chemistry and Pharmacology, The Ohio State University, Columbus, OH 43210, USA

[b]Center for Muscle Health and Neuromuscular Disorders, The Ohio State University and Nationwide Children's Hospital, Columbus, OH 43210

[c]Massachusetts General Hospital Cancer Center, Harvard Medical School, Charlestown, MA 02129; Department of Molecular Pathology and Regenerative Medicine, Massachusetts General Hospital, Charlestown, MA 02129; Harvard Stem Cell Institute, Cambridge, MA 02138, USA

Abstract

Satellite cells, also known as muscle stem cells, are responsible for skeletal muscle growth and repair in mammals. Pax7 and Pax3 transcription factors are established satellite cell markers required for muscle development and regeneration, and there is great interest in identifying additional factors that regulate satellite cell proliferation, differentiation, and/or skeletal muscle regeneration. Due to the powerful regenerative capacity of many zebrafish tissues, even in adults, we are exploring the regenerative potential of adult zebrafish skeletal muscle. Here, we show that adult zebrafish skeletal muscle contains cells similar to mammalian satellite cells. Adult zebrafish satellite-like cells have dense heterochromatin, express Pax7 and Pax3, proliferate in response to injury, and show peak myogenic responses 4–5 days post-injury (dpi). Furthermore, using a *pax7a*-driven GFP reporter, we present evidence implicating satellite-like cells as a possible source of new muscle. In lieu of central nucleation, which distinguishes regenerating myofibers in mammals, we describe several characteristics that robustly identify newly-forming myofibers from surrounding fibers in injured adult zebrafish muscle. These characteristics include partially overlapping expression in satellite cells and regenerating myofibers of two RNA-binding proteins Rbfox2 and Rbfoxl1, known to regulate embryonic muscle development and function. Finally, by analyzing *pax7a*; *pax7b* double mutant zebrafish, we show that Pax7 is required for adult skeletal muscle repair, as it is in the mouse.

*Corresponding author amacher.6@osu.edu.

Keywords

Pax transcription factors; Rbfox RNA-binding proteins; Muscle stem cells; Myogenesis; Muscle injury

INTRODUCTION

Analysis of frog leg muscles by electron microscopy led to the discovery of mononuclear cells located between the plasmalemma of muscle fibers and the surrounding basement membrane (Mauro, 1961). These cells, termed satellite cells based on their location, were hypothesized to play an important role in muscle regeneration and to function as adult muscle stem cells. Satellite cells have since been established as adult muscle stem cells; they are set aside early in development and remain as a largely quiescent cell population into adulthood (Bentzinger et al., 2012; Montarras et al., 2013). Satellite cells are activated in response to injury and give rise to differentiating myogenic precursor cells (MPCs) (Zammit et al., 2006), as well as other differentiated cell types including bone and brown fat (Asakura et al., 2001; Seale et al., 2008; Shefer et al., 2004).

Mammalian satellite cells reliably express the Pax7 transcription factor (Dumont et al., 2015; Seale et al., 2000). Additionally, Pax3 is expressed in satellite cells in certain mammalian skeletal muscle tissues such as the diaphragm (Montarras et al., 2005). Studies in mouse have identified several transcription factors that regulate satellite cell specification, proliferation, and differentiation (Bentzinger et al., 2012; Davis et al., 1987; Dumont et al., 2015; Rudnicki and Jaenisch, 1995; Weintraub et al., 1991). The most extensively studied of these is Pax7, which is required for murine satellite cell specification, maintenance, and adult skeletal muscle regeneration (Gunther et al., 2013; Seale et al., 2000; von Maltzahn et al., 2013).

Because zebrafish show a high capacity for regeneration, even in some adult tissues for which mammalian counterparts regenerate poorly (Poss et al., 2002; Reimer et al., 2008), the model has emerged as one in which to probe stem cell and regenerative biology. It is well established that larval zebrafish muscle contains satellite-like cells (Devoto et al., 2006; Feng et al., 2006; Gurevich et al., 2016; Knappe et al., 2015; Li et al., 2013; Nord et al., 2013; Otten et al., 2012; Seger et al., 2011; Siegel et al., 2013; Stellabotte et al., 2007; Windner et al., 2015), suggesting that they may also be present in adult muscle. Separate studies have noted the presence of Pax7-positive cells in adult zebrafish skeletal muscle and on isolated myofibers from adult zebrafish (Hollway et al., 2007; Tee et al., 2012; Zhang and Anderson, 2014); however, it is still unclear how similar zebrafish satellite-like cells are to mammalian satellite cells. Definitions of regeneration and repair vary in the literature; for this study, we use the term ‘regeneration’ to indicate replacement of a large portion of a tissue or organ and ‘repair’ to indicate the healing of a damaged portion of a tissue or organ. Zebrafish are competent in both regeneration (e.g., regeneration of the heart; Poss et al., 2002) and repair (e.g., healing after focal needle-stick injury; Gurevich et al., 2016; Knappe et al., 2015; März et al., 2011; Rowlerson et al., 1997; Seger et al., 2011). A few studies have examined skeletal muscle repair (Rowlerson et al., 1997; Tee et al., 2012) and regeneration

(Saera-Vila et al., 2015; Saera-Vila et al., 2016) after injury in adult zebrafish. The work from Rowlerson and colleagues (1997) was performed before the identification of satellite cell markers such as Pax7 and Pax3, and thus did not address whether adult zebrafish possess myogenic progenitor cells that function as satellite cells. A second study (Tee et al., 2012) observed Pax7-positive cells after needle-stick injury of adult zebrafish trunk musculature; however, only one time-point was examined and the contribution of Pax7-expressing cells to muscle repair was not assessed. Most recently, regeneration of extraocular muscle was found to occur through Fgf-regulated myocyte dedifferentiation that does not employ classic Pax7-positive satellite-like cells (Saera-Vila et al., 2015; Saera-Vila et al., 2016). Here, we have undertaken a comprehensive study to define the cells employed and steps involved during trunk skeletal muscle repair.

In addition to known satellite cell markers Pax7 and Pax3, there is active interest in identifying additional markers that may mark and/or regulate satellite cells and regenerating skeletal muscle. We have shown previously that Rbfox1l and Rbfox2, members of the Rbfox family of RNA binding proteins, are required for zebrafish embryonic muscle development and function (Gallagher et al., 2011). In mammals, the Rbfox family includes Rbfox1 (A2BP1; HRNBP1; FOX-1), Rbfox2 (RBM9; FOX-2) and the neural-specific Rbfox3 (NeuN; FOX-3) (Kuroyanagi et al., 2009). Rbfox proteins regulate alternative splicing in metazoans and their target intronic binding sites are extensively conserved among vertebrates (Gallagher et al., 2011; Lovci et al., 2013; Minovitsky et al., 2005; Yeo et al., 2007). Human RBFOX2 is required for human embryonic stem cell survival (Yeo et al., 2009) and promotes differentiation of pluripotent stem cells (Venables et al., 2013), suggesting a potential role for RBFOX2 in stem or progenitor cell regulation in multiple tissue types and organ systems. During zebrafish embryonic myogenesis, *rbfox2* is expressed in the presomitic mesoderm (a muscle progenitor domain) and newly-formed myotomal segments, but only weakly as muscle progenitors differentiate, whereas *rbfox1l* is expressed weakly in the progenitor domain and strongly in differentiating muscle cells (Gallagher et al., 2011). Previous studies corroborate muscle-specific embryonic expression of *rbfox1l* (Baxendale et al., 2009; Jin et al., 2003). Given these early expression patterns, we hypothesized that Rbfox2 and Rbfox1l may mark satellite-like cells and newly-forming myofibers, respectively, during injury-induced skeletal muscle repair in adult zebrafish.

In this study, we investigated the process of muscle repair in adult zebrafish skeletal muscle. Using transmission electron microscopy (TEM), immunohistochemistry, and transgenic reporter lines, we identify cells that closely resemble satellite cells within adult zebrafish skeletal muscle. Mechanical injury results in robust activation of Pax7 and *pax3a:GFP*-expressing satellite-like cells by 4–5 dpi. Acute EdU labeling of S-phase cells indicates that adult zebrafish satellite-like cells have proliferative potential, and perdurance of *pax7a*-driven GFP in new myofibers that form after muscle injury suggests that new muscle is at least partially derived from satellite-like cells. Lastly, our analysis of adult *pax7a*; *pax7b* double mutant zebrafish reveals that Pax7 function is required for adult skeletal muscle repair. Our findings further establish the adult zebrafish as a model to study satellite cell biology, and set the stage for future studies assessing Rbfox1l and Rbfox2 function in satellite cells, injury-induced repair, and muscle disease.

RESULTS

Pax7-expressing satellite-like cells are found within adult zebrafish skeletal muscle

Satellite cells were originally identified by electron microscopy (EM) in frog leg muscle as cells with dense heterochromatin (Mauro, 1961). Transmission electron microscopy (TEM) studies have also identified satellite cells in mammals (Seale et al., 2000). We performed TEM to determine whether cells resembling satellite cells are present in adult zebrafish skeletal muscle and find cells containing dense nuclear heterochromatin in both slow- and fast-twitch muscle fiber domains (Fig.1A, B; white arrowheads) that are easily distinguished from muscle fiber nuclei (myonuclei) (Fig. 1A, B; blue arrowheads). As in mammals (Seale et al., 2000), these satellite-like cells are located outside of the muscle fiber membrane and are surrounded by basal lamina (Fig. 1A′, B′; red arrows). In addition to morphological criteria, mammalian satellite cells also reliably express the Pax7 transcription factor (Seale et al., 2000). Previous studies have shown that Pax7-positive cells are present in larval zebrafish and are activated in response to injury and under disease conditions (Berger et al., 2010; Knappe et al., 2015; Seger et al., 2011). As described previously (Hollway et al., 2007; Tee et al., 2012), we also find Pax7-positive cells in adult zebrafish muscle (Fig. 1C, D). Pax7-positive cells are located beneath the basal lamina of the surrounding basement membrane (Fig. 1C–C‴) and external to the muscle membrane, which is marked in a Dystrophin FlipTrap insertion line, *dmd*^{ct90aGt}, that expresses a functional Dystrophin-Citrine fusion protein (Trinh et al., 2011) (Fig. 1D, D′). These data show that satellite-like cells in adult zebrafish express well-described satellite cell markers and are located in positions consistent with the location of satellite cells in other organisms (Bentzinger et al., 2012).

To evaluate the *pax7a:GFP*^{i131} BAC transgenic zebrafish line (Seger et al., 2011) as a marker for adult satellite-like cells, we examined overlap of Pax7 and *pax7a:GFP* expression in uninjured muscle sections (Fig. S1A–B″). As expected, almost all Pax7-positive cells express the *pax7a:GFP* transgene (98%; 302/308 cells; n=3). The converse comparison reveals that although the majority of *pax7a:GFP* transgene-expressing cells express Pax7 (72%; 302/422 cells; n=3), some are Pax7-negative (28%; 120/422 cells; n=3), possibly reflecting GFP perdurance, ectopic transgene expression, or cytoplasmic cellular protrusions for which the nucleus is out of the plane of section. To further clarify, we performed experiments to assess overlap of *pax7a:GFP*, Pax7, and DAPI labeling (Fig. S1C–D‴). Only 11% of *pax7a:GFP*-positive cells lack a DAPI-positive nucleus (42/398 cells; n=3) and thus likely represent cytoplasmic protrusions of cells for which nuclear expression cannot be assessed. Of the remaining *pax7a:GFP*-positive, DAPI-positive cells, the majority are Pax7-positive (70%; 248/356 cells; n=3); those that are Pax7-negative (30%; 108/356 cells; n=3) likely reflect GFP perdurance or ectopic transgene expression. Finally, virtually all Pax7-positive cells are DAPI-positive (253/255 cells; n=3) (Fig. 1C–C‴), further validating Pax7 as a bona fide satellite-like cell nuclear marker.

We find that the *pax3a:GFP*^{i150} BAC transgene (Seger et al., 2011) is also expressed in adult zebrafish satellite-like cells (Fig. S2). In uninjured adult muscle, a large fraction of Pax7-expressing cells express the *pax3a:GFP* transgene (90%; 75/84 cells; n=3), and conversely, a

majority of *pax3a:GFP*-expressing cells also express Pax7 (67%; 75/112 cells; n=3) (Fig. S2C, C′, C‴, mustard arrowheads). Although we utilize *pax3a:GFP* and *pax7a:GFP* transgenes as satellite-like cell markers in this work, we note that both are also expressed in non-myogenic cells in the skin (*pax3a:GFP* expression at the outer edge in Fig. S2A; *pax7a:GFP* expression at the outer edge in Fig. S2B) and spinal cord (Fig. S2A, arrowhead, for *pax3a:GFP* expression; Fig. S1D, for *pax7a:GFP* expression). In subsequent experiments, a nuclear label (Pax7, DAPI, or EdU) is usually included to assess and quantify marker and/or transgene expression.

Satellite-like cells are localized predominantly in the slow muscle domain

As in mammals, zebrafish slow muscle fibers contain many mitochondria compared to fast muscle fibers (Fig. 1A, B; an example indicated by a mustard arrow) (Schiaffino and Reggiani, 2011; Talbot and Maves, 2016; van Raamsdonk et al., 1980; Waterman, 1969), consistent with the distinct oxidative capacity of these two cell types. However, unlike in mammals, where slow and fast fiber types are often intermingled within muscles, zebrafish slow and fast fibers are segregated into spatially distinct domains (see Fig. 2A) (Bassett and Currie, 2003; Devoto et al., 1996; Elworthy et al., 2008; Jackson et al., 2015; Ju et al., 2003; Nord et al., 2014; Waterman, 1969). To identify slow and fast muscle domains, we used two transgenic lines: *Tg(smyhc1:GFP)*^{i104} that expresses GFP in slow muscle (Fig. 2C, D) (Elworthy et al., 2008) and *Tg(mylpfa:mCherry)*^{cz3327} that expresses mCherry in fast muscle (Fig. 2E, F) (Ignatius et al., 2012). These two transgenes robustly identify the majority of muscle fibers in the respective slow and fast muscle domains, but there are some non- or weakly-expressing cells at the border between them that may be intermediate fiber types (Elworthy et al., 2008; van Raamsdonk et al., 1980; Waterman, 1969). As expected, we find that satellite-like cells are sparsely localized throughout most of the adult myotome; however, they are enriched near the horizontal myoseptum, a slow muscle domain (schematized in Fig. 2A). To quantify the difference, we counted Pax7-positive cells within domains definitively labeled as slow muscle (Fig. 2C, D; cells to the left of the dotted blue line in the *symhc1:GFP*-positive domain) or fast muscle (Fig. 2E; cells to the right of the dotted brown line in the *mylpfa:mCherry*-positive domain) and normalized to total myofiber number in each domain. We find that Pax7-positive cells are 21-fold enriched in slow muscle relative to fast muscle (Fig. 2B), with very few Pax7-positive cells seen deep within the ventral myotome, a fast muscle domain (Fig. 2F).

Mechanical injury of adult zebrafish skeletal muscle results in Pax7-positive satellite-like cell proliferation and a concomitant increase in Pax7-positive cells at the injury site

Pax7-expressing satellite cells are required for skeletal muscle regeneration after injury in mammals (Lepper et al., 2011; Sambasivan et al., 2011). To determine whether adult zebrafish satellite-like cells behave similarly, we injured tail skeletal muscle by a single needle stick as previously described (Rowlerson et al., 1997) in the ventral myotome, to avoid the dorsally-located spinal cord and the satellite-like cell populations near the horizontal myoseptum (Fig. 3A). Fish were sacrificed daily from 2–7 dpi to assess whether and when satellite-like cells are activated by skeletal muscle injury (Fig. 3A). We find that Pax7-positive satellite-like cells increase after injury, peaking at 4 dpi and declining thereafter (Fig. 3B; Fig. S3G). The increase in Pax7-positive cells in the injured region

contrasts sharply to the minimal number of Pax7-positive cells found within the same ventral myotome region of uninjured fish (see Fig. 2B, F″).

To assess proliferation after injury, we acutely labeled cells using EdU at each post-injury time-point and observed the greatest numbers of EdU-positive cells at 2 and 3 dpi (Fig. 3C; Fig. S3A–F, H). Consistent with the expectation that non-activated satellite cells are a quiescent, non-dividing population, few Pax7-positive cells show EdU label in uninjured fish (Fig. S2C′, C″, C‴, white arrowheads); by contrast, many Pax7-positive, EdU-positive cells are detected after injury, peaking at 3 dpi (Fig. 3D, E; Fig. S3A–F). Additionally, the percentage of Pax7-positive cells that are EdU-positive is nearly 50% at 2 dpi, ~35% at 3 dpi, and less than 10% by 4 dpi (Fig. 3F). Between 2 and 4 dpi, we observe a 3-fold increase in the number of Pax7-positive cells at the injury site (Fig. S3G), suggesting an expansion of the Pax7-expressing cell population as a result of proliferation during that timeframe. Taken together, these data show that Pax7-expressing satellite-like cells in adult zebrafish skeletal muscle proliferate locally and robustly after needle stick injury.

Most Pax7-positive satellite-like cells express pax3a:GFP during adult zebrafish skeletal muscle repair

After needle stick injury in the *pax3a:GFP*^{i150} transgenic line (Seger et al., 2011), we observe that *pax3a:GFP*-positive cell number, like Pax7-positive cell number, gradually increases at the injury site and peaks in parallel with Pax7-positive cells (Fig. S4A, B). By 5 dpi, we observe a localized and robust activation of *pax3a*:*GFP* expression at the injury site (Fig. S4D). Satellite-like cells that are Pax7-positive and *pax3a:GFP*-positive are found at the injury site during a time of peak satellite-like cell response (Fig. S4D, D′, white arrowheads; Fig. S5D, G, white arrowheads). Quantification at 4 dpi indicates that 94% of Pax7-positive cells are also *pax3a*:*GFP*-positive (Fig. S5G, white arrowheads, 544/575 total cells counted; n=3), whereas only 6% are *pax3a*:*GFP*-negative (Fig. S4D′, blue arrowheads; Fig. S5G, blue arrowheads, 31/575 total cells counted; n=3). Due to the cytoplasmic localization of GFP, it is difficult to accurately quantify the percentage of *pax3a*:*GFP*-positive cells that express Pax7 in sections (*pax3a:GFP*-positive, Pax7-negative cells are shown by purple arrowheads in Fig. S4D′ and Fig. S5G). Since a large fraction of Pax7-expressing cells in uninjured muscle also express *pax3a:GFP*, it is not surprising that we find that cells expressing both Pax7 and *pax3a*:*GFP* proliferate in response to injury (Fig. S5C, mustard arrowheads; Fig. S5D–G, mustard arrowheads in G; compare with proliferation of Pax7-positive cells in Figure 3). These data show that satellite-like cells expressing both Pax7 and *pax3a*:*GFP* increase in number near the injury site after skeletal muscle needle stick injury.

Myoblast- and/or myogenic precursor-like cells that express myf5:GFP and myoD:GFP are present during adult zebrafish skeletal muscle repair

At 4 dpi, we observe cells that are Pax7-negative, *pax3a:GFP*-positive, and EdU-positive at the injury site (Fig. S5C, brown arrowheads). We hypothesized that these cells may be derived from satellite-like cells that have down-regulated Pax7 (and are likely no longer actively transcribing *pax3a:GFP*) and thus represent proliferating myogenic precursor cell (MPC)-like cells or myoblasts that are progressing toward differentiation. In mammals,

MPCs and myoblasts express the myogenic regulatory factors Myod and Myf5 (Bentzinger et al., 2012), while late-stage myoblasts express Myogenin (Myog) as they differentiate into myofibers. To determine whether myoblasts are present after injury, we performed injury in the *myod:GFP*^{i124} BAC transgenic line (Seger et al., 2011). We find *myod:GFP*-positive cells at the injury site at 4 dpi, some of which label with an acute pulse of EdU, suggesting that injury induces a proliferating myoblast-like population in adult zebrafish (Fig. 4A–A‴, arrowheads). *myod:GFP*-positive cells make up 15%, on average, of the total proliferative population present at the injury site (4 dpi), slightly fewer than (but not significantly different from) the percentage of proliferating Pax7-positive cells present (25%; Fig. 4B–C). The number of cells expressing both *myod:GFP* and Pax7 is minor; the large majority of Pax7-positive cells are *myod:GFP*-negative (90%; Fig. 4B–B‴, white arrowheads; Fig. 4D), further suggesting the existence of a myogenic population of cells distinct from (or possibly derived from) the Pax7-expressing satellite-like cell population. Additionally, we further investigated the presence of myoblast-like cells by performing injury in adult zebrafish carrying two transgenes: -*80.0myf5:GFP*^{zf37} (*myf5*-driven GFP, hereafter '*myf5:GFP*'; Chen et al., 2007) and *myog:H2B-mRFP* (*myog*-driven H2B (nuclear)-mRFP; Tang et al., 2016) (Fig. 4E). At 5 dpi, we find *myf5:GFP*-positive cells at the injury site, some of which are also *myog:H2B-mRFP*-positive (Fig. 4E–E″). The former are presumptive myoblasts or MPCs, whereas the latter may be late-stage myoblasts or newly-forming myofibers in which *myf5*-driven GFP perdures (Fig. 4E″, arrowheads). These data establish the presence of a proliferating myoblast-like population post-injury in adult zebrafish skeletal muscle.

Rbfox2 and Rbfox1l RNA-binding proteins are differentially expressed in Pax7-positive satellite-like cells during adult muscle repair

We previously showed that zebrafish *rbfox1l* and *rbfox2* genes are critical for embryonic skeletal muscle development and function (Gallagher et al., 2011) and hypothesized that they may also play important roles in adult skeletal muscle satellite-like cells. We generated antibodies against Rbfox1l and Rbfox2, and verified specificity by western blot of wild-type and Rbfox-depleted embryo extracts (Fig. S6A). In uninjured adult muscle, we find that Rbfox2 is expressed prominently in Pax7-positive cells (Fig. S6B–B″; white arrowheads) and in a minor subset of other nuclei (Fig. S6B–B″; gray arrowheads). Interestingly, some cells within the myotome have nuclear-localized Rbfox2, while in other cells Rbfox2 is cytoplasmic (Fig. S6E). Since Rbfox2 localizes with Pax7 in the nucleus of satellite-like cells (Fig. S6B–B″) we infer that cytoplasmic Rbfox2 marks other, non-myogenic cell types (such as blood or immune cells). In contrast, Rbfox1l is expressed in a subset of Pax7-positive cells (Fig. S6C–C″; white arrowheads) but more prominently in most, if not all, *myog:H2B-mRFP*-positive adult myofibers (Fig. S6D–D″), consistent with known muscle-specific *rbfox1l* expression (Baxendale et al., 2009; Gallagher et al., 2011). In uninjured muscle, Rbfox1l is consistently localized to the nucleus, seen by strong overlap with DAPI (Fig. S6F).

To assess Rbfox expression during muscle repair, we performed immunohistochemistry to detect Rbfox1l and Pax7 or Rbfox2 and Pax7 on adjacent sections at post-injury time-points 2–7 dpi (Fig. 5A). Rbfox1l is robustly expressed at the height of the satellite-like cell response (4 dpi; Fig. 5B). The absolute number of Pax7-positive, Rbfox1l-positive cells at

the injury site ranges from 10–35 cells, with no significant differences observed among post-injury time-points (Fig. 5B; magnified 4 dpi example shown in Fig. 5C–C″; purple arrowheads). Between 2–7 dpi, the percentage of Pax7-positive cells that are Rbfox1l-positive ranges between 28–43%, with no significant difference observed among post-injury time-points (Fig. 5D). Rbfox2 expression also peaks at 4 dpi, and precedes Rbfox1l expression as deduced by examining adjacent sections (Fig. 5B, E; Fig. 5F–F″; purple arrowheads). The absolute number of Pax7-positive, Rbfox2-positive cells at the injury site ranges from 34–101 cells, with the greatest number observed at 3 and 4 dpi (Fig. 5E), consistent with Pax7-positive cell response post-injury. In contrast with Rbfox1l, post-injury Rbfox2 expression closely mirrors that of Pax7; almost all (98–99.5%) Pax7-positive cells are Rbfox2-positive between 2–7 dpi, with no significant difference observed among time-points (Fig. 5G). We also observe Rbfox2-positive cells that are Pax7-negative (Fig. 5F–F″, blue arrowheads) and thus not satellite cells. These may represent differentiating myogenic cells, or even non-myogenic and/or immune or blood cells, as Rbfox2 is expressed quite broadly in zebrafish embryos (Gallagher et al, 2011) and in lymphocytic B-cells and hematopoietic progenitor cells in mammals (Ponthier et al., 2006). These data show that although RNA-binding proteins Rbfox1l and Rbfox2 are both expressed in quiescent and activated satellite-like cells at some level, Rbfox2 is more prevalent in satellite-like cells than Rbfox1l under both conditions. Additionally, during skeletal muscle repair, Rbfox2 expression precedes Rbfox1l expression at the injury site.

Rbfox1l, in contrast to Rbfox2, is expressed in differentiating muscle cells after injury

We hypothesized that Rbfox-expressing non-satellite cell populations might represent differentiating myogenic cells. To test this, we analyzed Rbfox1l expression post-injury in the *myog:H2B-mRFP* transgenic line (Fig. 6; myonuclei labeled in red). We find *myog:H2B-mRFP*-expressing cells at the injury site starting largely at 4 dpi and persisting thereafter, corresponding with onset of new myofiber formation (Fig. 6B). The absolute number of Rbfox1l; *myog:H2B-mRFP* double-positive cells similarly increases at the injury site (Fig. 6C, D). As in uninjured muscle (Fig. S6D″), Rbfox1l expression post-injury is found mainly within differentiating cells, with *myog:H2B-mRFP*-positive nuclei accounting for 71–95% of the total Rbfox1l-positive population between 4 and 7 dpi (Fig. 6E, 6F′–H′; white arrowheads). Interestingly, Rbfox1l is expressed in nuclei (Fig. 6F′–H′; white arrowheads) and cytoplasm (Fig. 6F′–H′; brown arrowheads) of newly-forming myofibers.

In similar experiments designed to characterize the Rbfox2-expressing non-satellite cell population, we observe that Rbfox2 is expressed in fewer myonuclei during skeletal muscle repair (Fig. 7A–C; F–H′, white arrowheads). Although the number of Rbfox2; *myog:H2B-mRFP* double-positive cells trends upward after 3 dpi and until 6 dpi, the data are not statistically significant among time-points (Fig. 7D). Additionally, *myog:H2B-mRFP*-positive myonuclei only account for 23–35% of the Rbfox2-expressing population between 4 and 7 dpi (Fig. 7E), with no significant difference observed among post-injury time-points. The Rbfox2-positive, *myog:H2B-mRFP*-negative cells we observe (see Fig. 7F′–H′ for magnified example at 4 dpi) likely include a combination of Pax7-positive satellite-like cells (Fig. 5F–G; Fig. S7A–C) and other cell types. Together, these data show that although there is overlap in Rbfox2 and Rbfox1l expression during post-injury repair, there are temporal

expression differences, with Rbfox2 expressed earlier and predominantly in Pax7-positive satellite-like cells and Rbfox1l expressed later in newly-forming myofibers.

New myofibers that form after injury in adult zebrafish skeletal muscle may be derived from Pax7-positive satellite-like cells

Because murine satellite cells proliferate in response to injury and give rise to new muscle during skeletal muscle regeneration (Bentzinger et al., 2012; Montarras et al., 2013), we investigated whether adult zebrafish satellite-like cells give rise to new myofibers during injury-induced repair. We used the *Tg(pax7a:GFP)*^{i131} BAC transgenic line, which drives GFP expression under control of *pax7a* regulatory elements (Seger et al., 2011), in combination with Pax7 antibody labeling, to infer lineage relationships between satellite-like cells and newly-forming myofibers (Fig. 8). As expected, we find satellite-like cells at the injury site expressing both *pax7a:GFP* and Pax7 protein at 5 dpi (Fig. 8B–B″, arrowheads point to examples). Other cells express GFP but no Pax7 protein (Fig. 8B–B″); these *pax7a:GFP*-positive cells also express Myosin heavy chain (MyHC) (Fig. 8C–E; shown at 4 dpi), which is robustly expressed in newly-forming, small diameter myofibers. Detection of *pax7a:GFP* in newly-forming myofibers (in the absence of Pax7 protein) suggests that *pax7a*-driven GFP may perdure in satellite-like cells that give rise to new myofibers. We observe a similar pattern in the *pax3a:GFP* transgenic line at 4 dpi (Fig. 8F), with weaker GFP expression in newly-forming myofibers that overlaps with differentiation marker *myog:H2B-mRFP* (Fig. 8F; white arrowheads). Additionally, we note that most of the newly forming myofibers in adult zebrafish have peripheral nuclei, and only in rare cases is central nucleation observed (Fig. 8F″, blue arrowhead). These observations implicate satellite-like cells as a source of new muscle during adult zebrafish skeletal muscle repair.

Pax7 is required for skeletal muscle repair in adult zebrafish

Given that Pax7 is necessary for proper muscle development and regeneration in mammals (Gunther et al., 2013; Oustanina et al., 2004; Seale et al., 2000; von Maltzahn et al., 2013), we investigated whether Pax7 is required for adult zebrafish muscle repair. Due to a teleost-specific genome duplication event, the zebrafish has two *pax7* genes: *pax7a* and *pax7b*. Because *pax7a* and *pax7b* are both expressed in larval and/or adult zebrafish satellite-like cells and are implicated in repair and/or regeneration (Devoto et al., 2006, Feng et al., 2006, Gurevich et al., 2016; Hollway et al., 2007, Knappe et al., 2015; Li et al., 2013; Nord et al., 2013; Otten et al., 2012; Pipalia et al., 2016; Seger et al., 2011; Siegel et al., 2013; Stellabotte et al., 2007; Windner et al., 2015; this study), we made loss-of-function mutations in both genes (Fig. 9A, B). *pax7a* frame-shifting mutants (*pax7a*^{oz19} and *pax7a*^{oz23}) are Pax7 protein null by immunohistochemistry (Fig. S8A–B), are viable, and show no obvious defects in skeletal muscle repair at 5 dpi (Fig. S8C–D). Similarly, *pax7b*^{oz32} homozygous mutants display no significant difference in new myofiber formation at 4 dpi, compared to wild-type siblings (Fig. S9). To fully investigate Pax7 function in zebrafish muscle repair, we generated the *pax7a*^{oz23}; *pax7b*^{oz32} double mutant. *pax7a*^{oz23}; *pax7b*^{oz32} double mutants have pigmentation defects and survive to adulthood, consistent with recently published observations (Nord et al., 2016). Using the needle-stick injury paradigm, we find dramatic defects in adult skeletal muscle repair in *pax7a*; *pax7b* double mutants (Fig. 9). At 4 dpi, newly-forming MyHC-positive, Rbfox1l-positive myofibers are

readily apparent at the injury site in wild-type adults (Fig. 9C; *pax7a*$^{+/-}$; *pax7b*$^{+/-}$ sibling control). In contrast, we observe a near-complete absence of Rbfox1l and MyHC labeling at the injury site in *pax7a*$^{-/-}$; *pax7b*$^{-/-}$ double mutants (Fig. 9D). We counted myofibers in 75 μm^2 regions within the injury site and find on average only 4 newly-forming myofibers in *pax7a*$^{-/-}$; *pax7b*$^{-/-}$ double mutants compared to an average of 45 newly-forming myofibers per 75 μm^2 within the injury site in *pax7a*$^{+/-}$; *pax7b*$^{+/-}$ sibling controls (n=2 adults per genotype; $p<0.01$, Student's t-test; 176 total myofibers counted in *pax7a*$^{+/-}$; *pax7b*$^{+/-}$, 15 total myofibers counted in *pax7a*$^{-/-}$; *pax7b*$^{-/-}$). These data reveal that Pax7 function is required for adult zebrafish skeletal muscle repair.

DISCUSSION

Muscle injury induces satellite-like cell activation and muscle repair in adult zebrafish skeletal muscle

The discovery of Pax7 as a reliable marker for satellite cells in mouse (Seale et al., 2000) has allowed investigators to examine whether similar cells are present in other model systems. Building on the identification of Pax7-positive satellite-like cells in larval and adult zebrafish (Berger et al., 2010; Hollway et al., 2007; Knappe et al., 2015; Seger et al., 2011; Siegel et al., 2013; Tee et al., 2012; Zhang and Anderson, 2014), we investigated whether adult zebrafish possess satellite-like cells that function in skeletal muscle repair. We find cells situated within the basal lamina that contain dense heterochromatin, express Pax7, proliferate in response to injury, and likely give rise to new myofibers during adult skeletal muscle repair, all properties of satellite cells in mammals. Additionally, we have identified that Rbfox2 and Rbfox1l are expressed predominantly in satellite-like cells and newly-forming myofibers, respectively, during the muscle repair process (Fig. 10A, B). Overall, we find Pax7, *pax3a:GFP* and Rbfox2 are expressed and EdU is incorporated during the time of progenitor cell expansion and proliferation, while Rbfox1l and *myog:H2B-mRFP* are expressed during later stages of myofiber differentiation during adult zebrafish skeletal muscle repair (Fig. 10B). A summary of markers and their relative expression (or incorporation, for EdU) levels during the post-injury time-course is depicted in Fig. 10B. Our findings illustrate that the zebrafish is a suitable vertebrate model system to study adult satellite cells and skeletal muscle repair.

Zebrafish adult muscle repair shares similarities with larval skeletal muscle repair

Previous studies in larval stage zebrafish revealed a population of Pax7-positive satellite-like cells (Berger et al., 2010; Knappe et al., 2015; Seger et al., 2011). Additionally, *pax7a*-driven GFP expression has been detected in cells concentrated at injury sites within 24–48 hours post injury of larval zebrafish at 4–5 days post-fertilization (dpf) (Knappe et al., 2015; Seger et al., 2011) and 7 dpf (Knappe et al., 2015). Similarly, we show that Pax7-expressing cells in adult zebrafish muscle increase after injury, peaking at 4 dpi and then declining sharply; this brief window of satellite cell expansion was not described in a previous adult study (Tee et al., 2012) because the time-point examined (7 dpi) occurs after the transient period of satellite cell expansion. Also similar to our adult findings, larval myofibers express *pax7a:GFP* after cardiotoxin injury at 4–5 dpf (Seger et al., 2011) and after extensive needle-stick injury (using a wider-bore needle) at 4 and 7 dpf (Knappe et al., 2015), suggesting that

pax7a-expressing zebrafish satellite-like cells contribute to new myofiber formation after injury at both larval and adult stages. A previous study found that a large injury (in contrast to small focal injury) is needed to induce *pax7a:GFP* expression in myofibers during larval muscle repair (Knappe et al., 2015). Although it is possible that our adult needle stick paradigm causes more extensive injury than focal injury in larval fish (Knappe et al., 2015), we note that the *pax7a:GFP* transgenic line used by Knappe and colleagues (2015) is distinct from the line used in the cardiotoxin study (Seger et al., 2011) and our current study. Future adult injury studies in both transgenic lines, that incorporate both small and large injuries will aid in addressing potential differences. In all these studies, GFP perdurance in newly-forming myofibers was used to infer that they are derived from *pax7a:GFP*-expressing satellite-like cells, thus differences between lines, injury paradigms, or adult and larval programs, could contribute to differences among studies. CreER-based lineage tracing approaches will more definitively address the extent to which Pax7-expressing cells contribute to new muscle after injury.

Injury-induced skeletal muscle repair in adult zebrafish: the use of stem/progenitor cells versus dedifferentiation

Our findings indicate that adult zebrafish possess satellite-like cells that function like mammalian satellite cells during skeletal muscle repair. Although *pax7*-driven GFP protein perdurance supports the idea that satellite-like cells contribute to new muscle after injury, it is not a definitive demonstration, and it is possible that new muscle forms by satellite cell-independent mechanisms. Some adult zebrafish tissues, like heart, fin, extraocular muscle, and retina, regenerate via dedifferentiation of mature cell types without using a specific precursor population (Geurtzen et al., 2014; Jopling et al., 2010; Knopf et al., 2011; Poss et al., 2002; Ramachandran et al., 2010; Saera-Vila et al., 2015; Saera-Vila et al., 2016; Sousa et al., 2011; Stewart et al., 2012; Wan et al., 2012). Particularly relevant to our study, post-injury regeneration of adult extraocular skeletal muscle uses dedifferentiation (Saera-Vila et al., 2015; Saera-Vila et al., 2016), demonstrating that some skeletal muscle types are repaired using satellite cell-independent mechanisms. However, another study using Cre/lox-based lineage tracing approaches found that dedifferentiation does not occur during regeneration of larval zebrafish tail muscle following amputation (Rodrigues et al., 2012). Additionally, recent studies have described larval zebrafish trunk muscle progenitor cell populations that contribute to new muscle fibers during repair after needle-stick injury (Gurevich et al., 2016; Pipalia et al., 2016). Using lineage tracing, Gurevich and colleagues (2016) found no evidence for dedifferentiation during larval trunk skeletal muscle repair. Our work strongly suggests that a local satellite-like cell population contributes to adult zebrafish skeletal muscle repair, but future lineage tracing studies will provide definitive evidence.

Pax3-expressing cells also contribute to muscle repair in both fish and mice

In this study, we have shown that zebrafish *pax3a:GFP*-positive satellite-like cells, like *pax7a:GFP*-positive satellite-like cells, are induced at the site of muscle injury and likely contribute to the repairing myotome. Because baseline *pax3a:GFP* transgene expression in larvae and adults is different, it is difficult to directly compare our results to a study performed in *pax3a*:*GFP* transgenic larval fish (Seger at el., 2011). In our study, the number

of *pax3a:GFP*-expressing cells is very low in uninjured adult muscle and robustly increases after injury; by contrast, there are already many *pax3a:GFP*-expressing cells in uninjured larval skeletal muscle and further increases are not observed after cardiotoxin-induced muscle injury (Seger et al., 2011). Additional larval studies are needed to distinguish whether the difference reflects variation in regenerative potential of *pax3a:GFP*-expressing cells or in differential expansion of the population.

In mammals, Pax3 is differentially expressed in satellite cells associated with different muscles; the mouse diaphragm contains more Pax3-expressing cells than Pax7-expressing cells, whereas tibialis anterior (TA) satellite cells primarily express Pax7 and not Pax3 (Kassar-Duchossoy et al., 2005; Montarras et al., 2005; Relaix et al., 2005). Coupled with knockout studies (Gunther et al., 2013; Relaix et al., 2005; Seale et al., 2000; von Maltzahn et al., 2013), the idea emerged that Pax3 and Pax7 may have both overlapping and distinct functions in murine satellite cells. In adult zebrafish, we find Pax7-expressing and *pax3a:GFP*-expressing cells in injured muscle, some of which express both Pax7 and *pax3a:GFP* (94% of Pax7-positive cells are also *pax3a:GFP*-positive), whereas others express only Pax7 or *pax3a:GFP*. Using GFP perdurance in *pax7a:GFP* and *pax3a:GFP* transgenic lines, we infer that both *pax7a:GFP*- and *pax3a:GFP*-expressing cells can generate new myofibers after injury; however, whether there is an independent population of Pax3-positive (but Pax7-negative) satellite-like cells that contributes to muscle repair after injury remains to be determined. As little is currently known about satellite cell sub-populations and whether they are differentially involved in skeletal muscle repair, future studies may provide novel insight into satellite cell heterogeneity and function.

Satellite-like cell localization in the zebrafish myotome and implications for the muscle stem cell niche and fiber type repair and regeneration

We have shown that adult zebrafish satellite-like cells are enriched within uninjured slow muscle, at the horizontal myoseptum, and at the boundary between fast and slow muscle domains. The differential localization of satellite-like cells is readily apparent due to the well-described spatial segregation of slow and fast muscle domains of the zebrafish myotome (Bassett and Currie, 2003; Devoto et al., 1996; Elworthy et al., 2008; Jackson et al., 2015; Ju et al., 2003; Nord et al., 2014; Waterman, 1969). In the zebrafish larval myotome, *pax7a*-expressing satellite-like cells are also concentrated largely around the edges of the slow muscle domain and at the horizontal myoseptum (Hollway et al., 2007; Knappe et al., 2015; Seger et al., 2011). We hypothesize that these areas represent a satellite-like cell niche. Intriguingly, previous work in the mouse also reported that more satellite cells associate with slow versus fast fibers (Collins et al., 2005; Shefer et al., 2006). Does the preferential association of satellite cells with slow muscle fibers have implications for regenerative capacity of slow versus fast fibers? Do resident satellite cells give rise to slow and fast muscle equivalently, or is there a hierarchical process (Wang et al., 2015)? Finally, do *pax7a* and/or *pax3a*-expressing satellite-like cell populations differentially contribute to fast and slow muscle? Studies that employ lineage-tracing methods and fiber type-specific transgenic lines will further investigate the relationship between satellite cell sub-populations and muscle fiber type regeneration.

Functional implications for Rbfox1l and Rbfox2 in skeletal muscle repair

It has long been appreciated that many molecular mechanisms regulating development of embryonic cells into differentiated tissue types are re-utilized during tissue regeneration and repair in adults. In this work, we show that Rbfox2 and Rbfox1l protein expression in the zebrafish adult myotome parallels what we previously described for *rbfox2* and *rbfox1l* transcript expression in embryos (Gallagher et al., 2011), with Rbfox2/*rbfox2* expression higher in less differentiated myogenic progenitor cells and Rbfox1l/*rbfox1l* expression increasing as cells differentiate into muscle. We hypothesize that Rbfox proteins regulate a muscle-specific splicing program that is employed first during embryonic muscle development and later in adult skeletal muscle satellite cells. Based on their expression patterns, we propose that Rbfox2 promotes satellite-like cell specification and/or maintenance, while Rbfox1l promotes satellite-like cell differentiation.

Do Rbfox proteins function in muscle regeneration and repair? RBFOX2 is required for human embryonic stem cell survival (Yeo et al., 2009) and promotes differentiation of human induced pluripotent stem cells (Venables et al., 2013). While Rbfox2 is expressed in many mammalian cell types including muscle, blood, embryonic, and neuronal cells (Dietrich et al., 2015; Underwood et al., 2005; Yeo et al., 2007), most Rbfox2 studies have focused on neuronal function (Gehman et al., 2012; O'Brien et al., 2012; Underwood et al., 2005; Weyn-Vanhentenryck et al., 2015; Yeo et al., 2007), though one recent study focused on Rbfox2 function in the mouse heart (Wei et al., 2015). However, whether Rbfox2 is expressed in mouse satellite cells, and/or functions during skeletal muscle development, growth, and/or regeneration has not been studied. The closest murine Rbfox1l homolog, Rbfox1, is primarily studied as a regulator of neuronal splicing (Gehman et al., 2011; Hamada et al., 2016; O'Brien et al., 2012; Weyn-Vanhentenryck et al., 2015), but is also expressed in heart and skeletal muscle (Kalsotra et al., 2008; Kiehl et al., 2001; Underwood et al., 2005). Surprisingly, conditional and partial Rbfox1 depletion in satellite cells does not affect muscle regeneration, with the caveat that only ~70% knockdown was achieved (Pedrotti et al., 2015). Recent work in C2C12 cells has identified a requirement for Rbfox1 and Rbfox2 in myotube differentiation in vitro (Runfola et al., 2015). Future studies in satellite cells in vivo and during regeneration may shed light on potential roles for Rbfox RNA-binding proteins in satellite cell regulation and skeletal muscle regeneration in vertebrates.

Do Rbfox proteins have non-nuclear functions?

We observe strong cytoplasmic Rbfox1l expression in newly-forming myofibers, which is intriguing since Rbfox proteins have been largely studied as regulators of alternative splicing, a nuclear function. We also observe cytoplasmic Rbfox2 in what appear to be non-muscle cells located between uninjured muscle fibers. Similarly, cytoplasmic Rbfox expression has been observed in neural tissue (Hamada et al., 2013; Lee et al., 2016), in germ cells (Carreira-Rosario et al., 2016), and various cell lines (Lee et al., 2009; Nakahata and Kawamoto, 2005), and a recent study has identified a role for cytoplasmic Rbfox1 in cortical development (Hamada et al., 2015). Since *rbfox* transcripts themselves are also targets of alternative splicing (Baraniak et al., 2006; Damianov and Black, 2010; Dredge and Jensen, 2011; Lee et al., 2009; Nakahata and Kawamoto, 2005; Yang et al., 2008), it is

possible that cytoplasmic Rbfox1l reflects post-transcriptional auto-regulation that tunes the level of Rbfox1l-regulated splicing events in the nucleus. Alternatively, or perhaps additionally, Rbfox1l may have cytoplasmic function(s) that influence transcript stability, localization, and/or translation as has been described for other RNA binding proteins (RBPs) (Blech-Hermoni and Ladd, 2013; Darnell and Richter, 2012). There is precedent for RNA-binding proteins having dual roles in both the nucleus and cytoplasm, as has been reported for *Drosophila* ELAV proteins (HuB, C, and D) (Bolognani and Perrone-Bizzozero, 2008; Fukao et al., 2009; Zhu et al., 2006). Indeed, recent work shows that RBFOX1/Rbfox1 may promote mRNA stability in mammals (Ray et al., 2013; Lee et al., 2016); for example, cytoplasmic Rbfox1 has been shown to regulate expression of autism-associated genes by binding neuronal transcript 3′ UTRs at sites that overlap significantly with miRNA binding sites (Lee et al., 2016). Additionally, regulation by Rbfox1 has been observed at the level of translation, whereby *Drosophila* Rbfox1 represses translation of transcripts containing 3′UTR Rbfox binding elements (Carreira-Rosario et al., 2016). Interestingly, Rbfox2 can regulate miRNA biogenesis by binding to miRNA precursors in mammalian cells (Chen et al., 2016). Taken together, we conclude that Rbfox proteins have important and conserved cellular regulatory functions in both the nucleus and cytoplasm.

Is Pax7 function in adult skeletal muscle repair conserved among vertebrates?

Several studies have established that Pax7 is required for proper adult skeletal muscle regeneration (Gunther et al., 2013; Oustanina et al., 2004; von Maltzahn et al., 2013), though another study indicated that Pax7 is dispensable (Lepper et al., 2009). The former studies found that regeneration was impaired after cardiotoxin injury in *Pax7* mutants, especially after multiple rounds of injury (Gunther et al., 2013; Oustanina et al., 2004; von Maltzahn et al., 2013). In our study, we have shown that *pax7a*; *pax7b* double mutant zebrafish are defective in adult skeletal muscle repair, revealing that *pax7* function is conserved during skeletal muscle regeneration in mice and zebrafish.

Is impaired regeneration in *Pax7* knockout mice due to a diminished satellite cell population or a diminished ability of satellite cells to participate? Pax7 is required for satellite cell maintenance in adult mice, as conditional knockout of Pax7 results in decreasing numbers of satellite cells over time (Gunther et al., 2013; von Maltzahn et al., 2013). However, it is unclear from these studies whether the few remaining satellite cells are able to proliferate and mount a satellite cell response post-injury, as satellite cell numbers were assessed at later post-injury time-points when regeneration is normally complete. Intriguingly, a previous study has reported that Pax7-lacZ-positive cells actually increase after injury in adult *Pax7* knockout mice (Oustanina et al., 2004), suggesting that satellite cells may be able to proliferate post-injury, but are unable to properly differentiate. Whether Pax7 is required for proliferation and/or maintenance of satellite cells or for satellite cell differentiation remains to be confirmed. Future work in both mice and fish will resolve which aspects of regeneration are controlled by Pax7.

EXPERIMENTAL PROCEDURES

Zebrafish Strains and Maintenance

Zebrafish strains were maintained according to The Ohio State University Institutional Animal Care and Use Committee (IACUC). Adult zebrafish between 2 and 6 months of age were used in our experiments, except in Figure 4E–E″ where the fish were 12 months old. Three to five adult zebrafish (of random sex) were used in experiments shown in Figs. 1, 2, and 8. Two adult zebrafish (of random sex) were used for each time-point and/or genotype in injury time-course experiments (Figs. 3, 5, 6, 7 and supplements to these figures), *pax7a; pax7b* double mutant analysis (Fig. 9, S8, S9), and Fig. 4 A–D (3 adults were analyzed in Fig. 4E). Zebrafish lines used were the AB wildtype strain, the BAC transgenic lines *TgBAC(pax3a:GFP)*^{i150} and *TgBAC(pax7a:GFP)*^{i131} (Seger et al., 2011), the *dmd*^{ct90aGt} transgenic insertion line that expresses Dystrophin-Citrine fusion protein (Trinh et al., 2011) and is referred to as Dystrophin FlipTrap in our work, *Tg(smyhc1:EGFP)*^{i104} (Elworthy et al., 2008), *Tg(mylpfa:mCherry)*^{cz3327} (Ignatius et al., 2012), *TgBAC(myod:GFP)*^{i124} (Seger et al., 2011), *Tg(-80.0myf5:EGFP)*^{zf37} (Chen et al., 2007), *Tg(acta1:GFP)*^{zf13} (also known as *alpha-actin:GFP*; Higashijima et al., 1997), and *Tg(myog:H2B-mRFP)* (Tang et al., 2016). *pax7a*^{oz19}, *pax7a*^{oz23}, and *pax7b*^{oz32} mutant zebrafish were generated in this study (see below). All mutant experiments were performed on zebrafish derived from F2 or later filial generation incrosses. The allele combination used for double mutant analysis was *pax7a*^{oz23}; *pax7b*^{oz32}.

Needle-stick injury procedure

Needle-stick injury was performed as previously described (Rowlerson et al., 1997). Adult zebrafish were anesthetized with Tricaine (0.004% diluted in fish system water), and muscle injury was performing by inserting and withdrawing a 27 gauge needle (0.4 mm) into the ventral myotome of the post-anal tail. Ventral myotome injury was performed to avoid damaging satellite-like cell populations at the horizontal myoseptum and the spinal cord. Zebrafish were returned to fresh water and monitored after injury. Zebrafish lacking full recovery (e.g. showing excessive bleeding and/or lethargic swimming) were euthanized. Injured zebrafish were housed and fed per normal protocols for 2 to 7 dpi until analysis.

Rbfox1l and Rbfox2 antibody production

Using Genomic Antibody Technology (SDIX LLC), polyclonal antibodies were raised in rabbits against divergent N-terminal regions of zebrafish Rbfox1l and Rbfox2. For anti-Rbfox1l, an immunogen of 81 amino acids spanning positions 30–110 was affinity purified and validated by ELISA against recombinant Rbfox1l protein. For anti-Rbfox2, an immunogen of 80 amino acids spanning positions 34–113 was affinity purified and validated by ELISA against recombinant Rbfox2 protein. Immunogenic peptides are:

Rbfox1l Immunogen sequence:
GAAAQEAGPGNGDPSLPQVYAPPPSYPPPGQAPPTPAARLPPLDFSAAHPNSE YADHHQLRV YQGPQHDGTESITASNTDD

Rbfox2 Immunogen sequence:
PPPQNGLSLEFSSGGGGSSVYSSSGQTEAVAGTSSGASNPSTQLSDASPQPDNQ LVLVSNAV AIREDSSEAKGTPKRLHV

Rbfox1l and Rbfox2 antibody validation

Zebrafish Rbfox1l and Rbfox2 polyclonal antibodies were validated by immunoblot analysis of embryo lysates from uninjected wild-type and Rbfox1l- and/or Rbfox2-depleted morphant embryos. To obtain Rbfox-depleted morphant samples, *rbfox1l* and *rbfox2* splice-blocking morpholinos, 5′-GCATTTGTTTTACCCCAAACATCTG-3′ and 5′-TATAATGCTTTATATACCCCGAACA-3′, respectively, were injected into the yolk of 1-cell stage embryos as previously described (Gallagher et al., 2011) and raised at 28.5°C for 24 hours. Zebrafish embryos were manually dechorionated at the 24 hpf stage and rapidly pipetted in cold Cell Resuspension Buffer (116 mM NaCl, 2.9 mM KCl, 5.0 mM HEPES, pH 7.2, 0.1 mg/mL Soybean Trypsin Inhibitor, Complete Protease Inhibitor Cocktail [Roche]). Cell lysis was performed in 2X LDS Buffer (Life Technologies). Cell extract equivalent to 2 embryos was loaded per lane, electrophoresed, and transferred to PVDF membrane using the Iblot semi-dry transfer system (Invitrogen). The blot was first probed with anti-Rbfox2 primary antibody (1:2500) and AP-conjugated goat anti-rabbit secondary antibody (1:10,000), developed, stripped according to the Western Superstar protocol, and then re-probed with anti-Rbfox1l primary antibody (1:2500) and AP-conjugated goat anti-rabbit secondary antibody (1:10,000). Blots were developed using the Western Superstar Kit (Applied Biosystems) according to manufacturer protocol. A separate blot loaded with the same protein lysates was processed at the same time, probed with anti-alphaTubulin primary antibody (1:2500) and AP-conjugated anti-mouse secondary antibody (1:10,000).

pax7a and pax7b mutant generation

pax7a and *pax7b* zebrafish mutants were generated using previously described CRISPR methods (Talbot and Amacher, 2014). For *pax7a*, a guide RNA (gRNA) targeting Exon 2 was synthesized from the following CRISPR target sequence: GGCGGATAGACCCGGTCTCC. gRNA and Cas9 mRNA were co-injected into one-cell stage zebrafish embryos. Injected embryos were grown to adulthood, and progeny from wild-type outcrosses were screened to identify germline-transmitting founders. Two frame-shifting alleles were generated: *oz19* (10 base-pair insertion) and *oz23* (2 base-pair deletion) (see Fig. 9A). Genotyping for *oz19* was performed using *pax7a* forward 5′-TATCCGACCCTGTGTTATCTCCAGAC-3′ and reverse 5′-AATCGTTCACTCACCCTCGGTTTG-3′ primers. The $pax7a^{oz19}$ amplicon (147 bp) is distinguished from the wild-type amplicon (137 bp) by size on an agarose gel. Genotyping for *oz23* was performed using *pax7a* forward 5′-GGTCAAGGTCGAGTCAATCAAC-3′ and reverse 5′-AGCTGAACATCCCTGGATTCTC-3′ primers. AvaII digestion cuts the $pax7a^{oz23}$ amplicon into two products (300 bp, 176 bp), whereas the wild-type amplicon is not cut (478 bp). For *pax7b*, a guide RNA targeting Exon 2 was synthesized from the following CRISPR target sequence: GGATTTTGGACACGCAGCCA. A 1 bp frame-shifting allele, *oz32*, was generated (see Fig. 9A). Genotyping for *oz32* was performed using *pax7b* forward 5′-CATCAATGGCAGGCCTTTGC-3′ and reverse 5′-

CACACCCCGTCCTTCAACAG-3′ primers. Fnu4HI digestion cuts the wild-type amplicon into two products (425 bp, 110 bp), whereas the *pax7b*^{oz32} amplicon is not cut (534 bp).

Tissue processing and immunohistochemistry

Adult zebrafish were anesthetized with Tricaine (0.004% diluted in fish system water) and fixed overnight in 4% PFA by immersion fixation. The following day, tail skeletal muscle was isolated using a razor blade and washed in a glass vial containing 1X PBS for 10 minutes. Subsequently, 1X PBS solution was replaced with a solution of 30% sucrose in 1X PBS (cryopreservation), and samples were placed on a rocker for approximately 3 hours at room temperature until tissue samples sank to the bottom of vial. Muscle tissue was embedded in OCT (Sakura Finetek), frozen on a slab of dry ice, and cut using a Microm 550 cryostat into 25 μm thick cryosections onto Superfrost Plus Microscope slides (Thermo Fisher Scientific) and stored at −20°C. Sections of the injury area anterior to and including the needle lesion were collected. Immunohistochemistry was performed as previously described for adult zebrafish tissue sections (Berberoglu et al., 2009; Berberoglu et al., 2014). Briefly, slides were washed in 1X PBS at room temperature to rehydrate tissue and remove OCT, and then incubated in PBS + 0.5% Triton X-100 for 10 minutes to permeabilize membranes. Slides were washed in 1X PBS for 15 minutes, blocked in PBS + 3% bovine serum albumin (BSA) for 1–2 hours at room temperature, and incubated in primary antibody overnight at 4°C. The following day, slides were washed 2–3 times with 1X PBS over 1 hour, followed by PBS + 0.1% Triton X-100 for 10 minutes. Slides were then incubated in secondary antibody (diluted in PBS + 0.1% Triton X-100) for 2 hours at room temperature. Slides were washed 2–3 times for 30 minutes in 1X PBS, mounted with fluorescent mounting medium (Dako), and coverslipped. In our experiments, anti-GFP antibody was used to amplify GFP signal.

The following primary antibodies were used at the indicated dilutions: mouse anti-Pax7 (DSHB; 1:20); chicken anti-GFP (ab13970, Abcam; 1:2000), rabbit anti-Rbfox2 (1:1000), rabbit anti-Rbfox1l (1:1000), rabbit anti-Laminin (L9393, Sigma; 1:100), mouse anti-MyHC (A4.1025, DSHB; 1:1000). The following Alexa Fluor secondary antibodies were used at 1:200 dilution: anti-chicken 488, anti-rabbit and anti-mouse 488, 568, and 647 (Thermo Fisher Scientific).

Intraperitoneal EdU injection to label S-phase cells

For EdU labeling experiments, adult zebrafish were injected intraperitoneally following Tricaine anesthetization with 20 uL of 10 mM EdU (5-ethynyl-2′-deoxyuridine; Life Technologies) diluted in 1X PBS. Zebrafish were returned to fresh water after injection and monitored for recovery from anesthesia. Fish that did not regain consciousness were euthanized per IACUC protocol. For EdU pulse experiments (acute EdU labeling), zebrafish were housed for 4 hours to allow for EdU incorporation before fixation and tissue processing as described above. For EdU labeling on tissue sections, the click-chemistry reaction was performed as described (Invitrogen Life Technologies). Following PBS + 0.5% Triton incubation and 15 minute 1X PBS wash (described above), a 10 minute incubation of EdU labeling solution (in the dark) is the optimal labeling time used in our experiments. Incubation is followed by a 15-minute wash with 1X PBS before blocking.

Transmission Electron Microscopy

Transmission electron microscopy was performed according to standard procedures set by the OSU Campus Microscopy & Imaging Facility. Methods were adapted for adult zebrafish skeletal muscle as follows. In brief, adult zebrafish were anesthetized and then decapitated to sacrifice. Skin was removed from tail muscle region of interest, and a transfer pipette was used to place a few drops of fixative (2% glutaraldehyde in 0.1M phosphate buffer, pH 7.4) onto the tissue. After a few minutes, tail muscle tissue was dissected out and fixed (same fixative) an additional 15 minutes (in a small dish). Tissue from both slow and fast-twitch muscle fiber domains was cut into small pieces (1mm × 2mm, to aid in orientation, using a fine scalpel) and fixed in vials overnight at 4°C. Samples were embedded using standard procedures for TEM, and thick sections were taken and stained with toluidine blue. Orientation was assessed, and thin sections (70–90 nm; cross-sections) were then taken from a smaller area of the block for labeling and imaging.

Confocal imaging, image processing, and statistical analyses

Samples were imaged using a Leica TCS SL point-scanning laser confocal inverted microscope or an Andor Revolution WD spinning disk laser confocal microscope system (Inverted Nikon TiE microscope). Confocal projection images (~15μm or narrower) and single confocal z-sections (0.5–1 μm) were used to assess co-localization of markers. For quantification, all cells counted had at least one marker localized to the nucleus to ensure accurate cell counts. Cells were counted manually on 2 sections from each of 2–3 adult zebrafish per genotype and/or time-point using NIH ImageJ. Cell counts over 2 sections were averaged per adult zebrafish; percentages of cells are reported based on an average of averages (for statistical comparisons). Numbers of cells counted in experiments are reported as absolute numbers (without averaging between sections). Graphpad Prism 7 was used for statistical analysis. Adobe Photoshop CS6 and NIH ImageJ were used for image processing. Student's t-test was performed for statistical comparison of two conditions. For injury time-course experiments, a One-Way ANOVA followed by Tukey's multiple comparisons test was performed. $p^{*}<0.05$, $p^{**}<0.01$, $p^{***}<0.001$.

Supplementary Material

Refer to Web version on PubMed Central for supplementary material.

Acknowledgments

This work was supported by intramural funds from the Ohio State University and Nationwide Children's Hospital Center for Muscle Health and Neuromuscular Disorders (CMHND), NIH grant R01GM117964 (to S.L.A.), and American Heart Association Grant #0825194F (T.L.G.). M.A.B. was supported by a CMHND-administered NIH/NINDS T32 training grant (NS077984) and by a Pelotonia Postdoctoral Fellowship. We thank Phillip Ingham for *pax7a:GFP*, *pax3a:GFP*, and *myod:GFP* BAC transgenic lines and for the *smyhc1:EGFP* line, and Le Trinh and Scott Fraser for the Dystrophin FlipTrap line. We thank Richard Montione and the OSU Campus Microscopy & Imaging Facility for TEM assistance, the Neuroscience Imaging Core for equipment and advice, Rightmire fish facility staff for excellent fish maintenance, Brittany Siegenthaler and Anne Witzky for genotyping assistance, and Anne Witzky and Duy Phan for antibody testing. Finally, we thank Amacher lab members, the CMHND "Muscle Group" research community, and Rightmire Zebrafish Groups for helpful discussions throughout the course of this study, and Denis Guttridge for reading and commenting on an early draft.

References

Asakura A, Komaki M, Rudnicki M. Muscle satellite cells are multipotential stem cells that exhibit myogenic, osteogenic, and adipogenic differentiation. Differentiation. 2001; 68:245–253. [PubMed: 11776477]

Baraniak AP, Chen JR, Garcia-Blanco MA. Fox-2 mediates epithelial cell-specific fibroblast growth factor receptor 2 exon choice. Mol Cell Biol. 2006; 26:1209–1222. [PubMed: 16449636]

Bassett DI, Currie PD. The zebrafish as a model for muscular dystrophy and congenital myopathy. Hum Mol Genet. 2003; 12:R265–270. [PubMed: 14504264]

Baxendale S, Chen CK, Tang H, Davison C, Hateren LV, Croning MD, Humphray SJ, Hubbard SJ, Ingham PW. Expression screening and annotation of a zebrafish myoblast cDNA library. Gene Expr Patterns. 2009; 9:73–82. [PubMed: 19007914]

Bentzinger CF, Wang YX, Rudnicki MA. Building muscle: molecular regulation of myogenesis. Cold Spring Harb Perspect Biol. 2012; 4(2) doi:pii: a008342. Review.

Berberoglu MA, Dong Z, Li G, Zheng J, Martinez LC, Peng J, Wagle M, Reichholf B, Petritsch C, Li H, Pleasure S, Guo S. Heterogeneously expressed fezf2 patterns gradient Notch activity in balancing the quiescence, proliferation, and differentiation of adult neural stem cells. J Neurosci. 2014; 34:13911–13923. [PubMed: 25319688]

Berberoglu MA, Dong Z, Mueller T, Guo S. fezf2 expression delineates cells with proliferative potential and expressing markers of neural stem cells in the adult zebrafish brain. Gene Expr Patterns. 2009; 9:411–422. [PubMed: 19524703]

Berger J, Berger S, Hall TE, Lieschke GJ, Currie PD. Dystrophin-deficient zebrafish feature aspects of Duchenne muscular dystrophy pathology. Neuromuscular Disorders. 2010; 20:826–832. [PubMed: 20850317]

Blech-Hermoni Y, Ladd AN. RNA binding proteins in the regulation of heart development. Int J Biochem Cell Biol. 2013; 45:2467–2478. [PubMed: 23973289]

Bolognani F, Perrone-Bizzozero NI. RNA-protein interactions and control of mRNA stability in neurons. J Neurosci Res. 2008; 86:481–489. [PubMed: 17853436]

Carreira-Rosario A, Bhargava V, Hillebrand J, Kollipara RK, Ramaswami M, Buszczak M. Repression of Pumilio protein expression by Rbfox1 promotes germ cell differentiation. Dev Cell. 2016; 36:562–571. [PubMed: 26954550]

Chen YH, Wang YH, Chang MY, Lin CY, Weng CW, Westerfield M, Tsai HJ. Multiple upstream modules regulate zebrafish myf5 expression. BMC Dev Biol. 2007; 3(7):1.

Chen Y, Zubovic L, Yang F, Godin K, Pavelitz T, Castellanos J, Macchi P, Varani G. Rbfox proteins regulate microRNA biogenesis by sequence-specific binding to their precursors and target downstream Dicer. Nucleic Acids Res. 2016; 44:4381–4395. [PubMed: 27001519]

Collins CA, Olsen I, Zammit PS, Heslop L, Petrie A, Partridge TA, Morgan JE. Stem cell function, self-renewal, and behavioral heterogeneity of cells from the adult muscle satellite cell niche. Cell. 2005; 122:289–301. [PubMed: 16051152]

Darnell JC, Richter JD. Cytoplasmic RNA-binding proteins and the control of complex brain function. Cold Spring Harb Perspect Biol. 2012; 4:a012344. [PubMed: 22723494]

Davis RL, Weintraub H, Lassar AB. Expression of a single transfected cDNA converts fibroblasts to myoblasts. Cell. 1987; 51:987–1000. [PubMed: 3690668]

Devoto SH, Melancon E, Eisen J, Westerfield M. Identification of separate slow and fast muscle precursor cells in vivo, prior to somite formation. Development. 1996; 122:3371–3380. [PubMed: 8951054]

Devoto SH, Stoiber W, Hammond CL, Steinbacher P, Haslett JR, Barresi MJ, Patterson SE, Adiarte EG, Hughes SM. Generality of vertebrate developmental patterns: evidence for a dermomyotome in fish. Evol Dev. 2006; 8:101–110. [PubMed: 16409387]

Dietrich JE, Panavaite L, Gunther S, Wennekamp S, Groner AC, Pigge A, Salvenmoser S, Trono D, Hufnagel L, Hiiragi T. Venus trap in the mouse embryo reveals distinct molecular dynamics underlying specification of first embryonic lineages. EMBO Rep. 2015; 16:1005–1021. [PubMed: 26142281]

Dredge BK, Jensen KB. NeuN/Rbfox3 nuclear and cytoplasmic isoforms differentially regulate alternative splicing and nonsense-mediated decay of Rbfox2. PLoS One. 2011; 6:e21585. [PubMed: 21747913]

Dumont NA, Wang YX, Rudnicki MA. Intrinsic and extrinsic mechanisms regulating satellite cell function. Development. 2015; 142:1572–1581. [PubMed: 25922523]

Elworthy S, Hargrave M, Knight R, Mebus K, Ingham PW. Expression of multiple slow myosin heavy chain genes reveals a diversity of zebrafish slow twitch muscle fibres with differing requirements for Hedgehog and Prdm1 activity. Development. 2008; 135:2115–2126. [PubMed: 18480160]

Feng X, Adiarte EG, Devoto SH. Hedgehog acts directly on the zebrafish dermomyotome to promote myogenic differentiation. Dev Biol. 2006; 300:736–746. [PubMed: 17046741]

Fukao A, Sasano Y, Imataka H, Inoue K, Sakamoto H, Sonenberg N, Thoma C, Fujiwara T. The ELAV protein HuD stimulates cap-dependent translation in a Poly(A)- and eIF4A-dependent manner. Mol Cell. 2009; 36:1007–1017. [PubMed: 20064466]

Gallagher TL, Arribere JA, Geurts PA, Exner CR, McDonald KL, Dill KK, Marr HL, Adkar SS, Garnett AT, Amacher SL, Conboy JG. Rbfox-regulated alternative splicing is critical for zebrafish cardiac and skeletal muscle functions. Dev Biol. 2011; 359:251–261. [PubMed: 21925157]

Gehman LT, Meera P, Stoilov P, Shiue L, O'Brien JE, Meisler MH, Ares M Jr, Otis TS, Black DL. The splicing regulator Rbfox2 is required for both cerebellar development and mature motor function. Genes Dev. 2012; 26:445–460. [PubMed: 22357600]

Gehman LT, Stoilov P, Maguire J, Damianov A, Lin CH, Shiue L, Ares M Jr, Mody I, Black DL. The splicing regulator Rbfox1 (A2BP1) controls neuronal excitation in the mammalian brain. Nat Genet. 2011; 43:706–711. [PubMed: 21623373]

Geurtzen K, Knopf F, Wehner D, Huitema LF, Schulte-Merker S, Weidinger G. Mature osteoblasts dedifferentiate in response to traumatic bone injury in the zebrafish fin and skull. Development. 2014; 141:2225–2234. [PubMed: 24821985]

Gunther S, Kim J, Kostin S, Lepper C, Fan CM, Braun T. Myf5-positive satellite cells contribute to Pax7-dependent long-term maintenance of adult muscle stem cells. Cell Stem Cell. 2013:S1934–5909. pii.

Gurevich DB, Nguyen PD, Siegel AL, Ehrlich OV, Sonntag C, Phan JM, Berger S, Ratnayake D, Hersey L, Berger J, Verkade H, Hall TE, Currie PD. Asymmetric division of clonal muscle stem cells coordinates muscle regeneration in vivo. Science. 2016; 353:aad9969. [PubMed: 27198673]

Hamada N, Ito H, Iwamoto I, Mizuno M, Morishita R, Inaguma Y, Kawamoto S, Tabata H, Nagata K. Biochemical and morphological characterization of A2BP1 in neuronal tissue. J Neurosci Res. 2013; 91:1303–1311. [PubMed: 23918472]

Hamada N, Ito H, Iwamoto I, Morishita R, Tabata H, Nagata K. Role of the cytoplasmic isoform of RBFOX1/A2BP1 in establishing the architecture of the developing cerebral cortex. Mol Autism. 2015; 6:56. [PubMed: 26500751]

Hamada N, Ito H, Nishijo T, Iwamoto I, Morishita R, Tabata H, Momiyama T, Nagata K. Essential role of the nuclear isoform of RBFOX1, a candidate gene for autism spectrum disorders, in the brain development. Sci Rep. 2016; 6:30805. [PubMed: 27481563]

Higashijima S, Okamoto H, Ueno N, Hotta Y, Eguchi G. High-frequency generation of transgenic zebrafish which reliably express GFP in whole muscles or the whole body by using promoters of zebrafish origin. Dev Biol. 1997; 192:289–299. [PubMed: 9441668]

Hollway GE, Bryson-Richardson RJ, Berger S, Cole NJ, Hall TE, Currie PD. Whole-somite rotation generates muscle progenitor cell compartments in the developing zebrafish embryo. Dev Cell. 2007; 12:207–219. [PubMed: 17276339]

Ignatius MS, Chen E, Elpek NM, Fuller AZ, Tenente IM, Clagg R, Liu S, Blackburn JS, Linardic CM, Rosenberg AE, Nielsen PG, Mempel TR, Langenau DM. In vivo imaging of tumor-propagating cells, regional tumor heterogeneity, and dynamic cell movements in embryonal rhabdomyosarcoma. Cancer Cell. 2012; 21:680–693. [PubMed: 22624717]

Jackson HE, Ono Y, Wang X, Elworthy S, Cunliffe VT, Ingham PW. The role of Sox6 in zebrafish muscle fiber type specification. Skelet Muscle. 2015; 5:2. [PubMed: 25671076]

Jin Y, Suzuki H, Maegawa S, Endo H, Sugano S, Hashimoto K, Yasuda K, Inoue K. A vertebrate RNA-binding protein Fox-1 regulates tissue-specific splicing via the pentanucleotide GCAUG. Embo J. 2003; 22:905–912. [PubMed: 12574126]

Jopling C, Sleep E, Raya M, Marti M, Raya A, Izpisúa Belmonte JC. Zebrafish heart regeneration occurs by cardiomyocyte dedifferentiation and proliferation. Nature. 2010; 464:606–609. [PubMed: 20336145]

Ju B, Chong SW, He J, Wang X, Xu Y, Wan H, Tong Y, Yan T, Korzh V, Gong Z. Recapitulation of fast skeletal muscle development in zebrafish by transgenic expression of GFP under the mylz2 promoter. Dev Dyn. 2003; 227:14–26. [PubMed: 12701095]

Kalsotra A, Xiao X, Ward AJ, Castle JC, Johnson JM, Burge CB, Cooper TA. A postnatal switch of CELF and MBNL proteins reprograms alternative splicing in the developing heart. Proc Natl Acad Sci USA. 2008; 105:20333–20338. [PubMed: 19075228]

Kassar-Duchossoy L, Glacone E, Gayraud-Morel B, Jory A, Gomes D, Tajbakhsh S. Pax3/7 mark a novel population of primitive myogenic cells during development. Genes & Development. 2005; 19:1426–1431. [PubMed: 15964993]

Kiehl TR, Shibata H, Vo T, Huynh DP, Pulst SM. Identification and expression of a mouse ortholog of A2BP1. Mamm Genome. 2001; 12:595–601. [PubMed: 11471052]

Knappe S, Zammit PS, Knight RD. A population of Pax7-expressing muscle progenitor cells show differential responses to muscle injury dependent on developmental stage and injury extent. Front Aging Neurosci. 2015; 7:161. [PubMed: 26379543]

Knopf F, Hammond C, Chekuru A, Kurth T, Hans S, Weber CW, Mahatma G, Fisher S, Brand M, Schulte-Merker S, Weidinger G. Bone regeneration via dedifferentiation of osteoblasts in the zebrafish fin. Dev Cell. 2011; 20:713–724. [PubMed: 21571227]

Kuroyanagi H. Fox-1 family of RNA-binding proteins. Cell Mol Life Sci. 2009; 66:3895–3907. [PubMed: 19688295]

Kwan KM, Fujimoto E, Grabher C, Mangum BD, Hardy ME, Campbell DS, Parant JM, Yost HJ, Kanki JP, Chien CB. The Tol2kit: A multisite gateway-based construction kit for Tol2 transposon transgenesis constructs. Dev Dyn. 2007; 236:3088–3099. [PubMed: 17937395]

Lee JA, Damianov A, Lin CH, Fontes M, Parikshak NN, Anderson ES, Geschwind DH, Black DL, Martin KC. Cytoplasmic Rbfox1 regulates the expression of synaptic and autism-related genes. Neuron. 2016; 89:113–128. [PubMed: 26687839]

Lee JA, Tang ZZ, Black DL. An inducible change in Fox-1/A2BP1 splicing modulates the alternative splicing of downstream neuronal target exons. Genes Dev. 2009; 23:2284–2293. [PubMed: 19762510]

Lepper C, Conway SJ, Fan CM. Adult satellite cells and embryonic muscle progenitors have distinct genetic requirements. Nature. 2009; 460:627–631. [PubMed: 19554048]

Lepper C, Partridge TA, Fan CM. An absolute requirement for Pax7-positive satellite cells in acute injury-induced skeletal muscle regeneration. Development. 2011; 138:3639–3646. [PubMed: 21828092]

Li YH, Chen HY, Li YW, Wu SY, Wangta-Liu, Lin GH, Hu SY, Chang ZK, Gong HY, Liao CH, Chiang KY, Huang CW, Wu JL. Progranulin regulates zebrafish muscle growth and regeneration through maintaining the pool of myogenic progenitor cells. Science Rep. 2013; 3:1176.

Lovci MT, Ghanem D, Marr H, Arnold J, Gee S, Parra M, Liang TY, Stark TJ, Gehman LT, Hoon S, Massirer KB, Pratt GA, Black DL, Gray JW, Conboy JG, Yeo GW. Rbfox proteins regulate alternative mRNA splicing through evolutionarily conserved RNA bridges. Nat Struct Mol Biol. 2013; 20:1434–1442. [PubMed: 24213538]

März M, Schmidt R, Rastegar S, Strähle U. Regenerative response following stab injury in the adult zebrafish telencephalon. Dev Dyn. 2011; 240:2221–2231. [PubMed: 22016188]

Mauro A. Satellite cell of skeletal muscle fibers. J Biophys Biochem Cytol. 1961; 9:493–495. [PubMed: 13768451]

Minovitsky S, Gee SL, Schokrpur S, Dubchak I, Conboy JG. The splicing regulatory element, UGCAUG, is phylogenetically and spatially conserved in introns that flank tissue-specific alternative exons. Nucleic Acids Res. 2005; 33:714–724. [PubMed: 15691898]

Montarras D, L'honore A, Buckingham M. Lying low but ready for action: the quiescent muscle satellite cell. FEBS J. 2013; 280:4036–4050. [PubMed: 23735050]

Montarras D, Morgan J, Collins C, Relaix F, Zaffran S, Cumano A, Partridge T, Buckingham M. Direct isolation of satellite cells for skeletal muscle regeneration. Science. 2005; 309:2064–2067. [PubMed: 16141372]

Nakahata S, Kawamoto S. Tissue-dependent isoforms of mammalian Fox-1 homologs are associated with tissue-specific splicing activities. Nucleic Acids Res. 2005; 33:2078–2089. [PubMed: 15824060]

Nord H, Burguiere A, Muck J, Nord C, Ahlgren U, von Hofsten J. Differentiation regulation of myosin heavy chains defines new muscle domains in zebrafish. Mol Biol Cell. 2014; 25:1384–1395. [PubMed: 24523292]

Nord H, Dennhag N, Muck J, von Hofsten J. Pax7 is required for establishment of the xanthophore lineage in zebrafish embryos. Mol Biol Cell. 2016; 27:1853–1862. [PubMed: 27053658]

Nord H, Nygard Skalman L, von Hofsten J. Six1 regulates proliferation of Pax7-positive muscle progenitors in zebrafish. J Cell Sci. 2013; 126:1868–1880. [PubMed: 23444384]

O'Brien JE, Drews VL, Jones JM, Dugas JC, Barres BA, Meisler MH. Rbfox proteins regulate alternative splicing of neuronal sodium channel SCN8A. Mol Cell Neurosci. 2012; 49:120–126. [PubMed: 22044765]

Otten C, van der Ven PF, Lewrenz I, Paul S, Steinhagen A, Busch-Nentwich E, Eichhorst J, Wiesner B, Stemple D, Strahle U, Furst DO, Abdelilah-Seyfried S. Xirp proteins mark injured skeletal muscle in zebrafish. PLoS One. 2012; 7:e31041. [PubMed: 22355335]

Oustanina S, Hause G, Braun T. Pax7 directs postnatal renewal and propagation of myogenic satellite cells but not their specification. EMBO J. 2004; 23:3430–3439. [PubMed: 15282552]

Pedrotti S, Giudice J, Dagnino-Acosta A, Knoblauch M, Singh RK, Hanna A, Mo Q, Hicks J, Hamilton S, Cooper TA. The RNA-binding protein Rbfox1 regulates splicing required for skeletal muscle structure and function. Human Molecular Genetics. 2015; 24:2360–2374. [PubMed: 25575511]

Pipalia TG, Koth J, Roy SD, Hammond CL, Kawakami K, Hughes SM. Cellular dynamics of regeneration reveals role of two distinct Pax7 stem cell populations in larval zebrafish muscle repair. Dis Model Mech. 2016; 9:671–684. [PubMed: 27149989]

Ponthier JL, Schluepen C, Chen W, Lersch RA, Gee SL, Hou VC, Lo AJ, Short SA, Chasis JA, Winkelmann JC, Conboy JG. Fox-2 splicing factor binds to a conserved intron motif to promote inclusion of protein 4.1R alternative exon 16*. Journal of Biological Chemistry. 2006; 281:12468–12474. [PubMed: 16537540]

Poss KD, Wilson LG, Keating MT. Heart regeneration in zebrafish. Science. 2002; 298:2188–2190. [PubMed: 12481136]

Ramachandran R, Fausett BV, Goldman D. Ascl1a regulates Müller glia dedifferentiation and retinal regeneration through a Lin-28-dependent, let-7 microRNA signaling pathway. Nat Cell Biol. 2010; 12:1101–1107. [PubMed: 20935637]

Ray D, Kazan H, Cook KB, Weirauch MT, Najafabadi HS, Li X, Gueroussov S, Albu M, Zheng H, Yang A, Na H, Irimia M, Matzat LH, Dale RK, Smith SA, Yarosh CA, Kelly SM, Nabet B, Mecenas D, et al. A compendium of RNA-binding motifs for decoding gene regulation. Nature. 2013; 499:172–177. [PubMed: 23846655]

Reimer MM, Sörensen I, Kuscha V, Frank RE, Liu C, Becker CG, Becker T. Motor neuron regeneration in adult zebrafish. J Neurosci. 2008; 28:8510–8516. [PubMed: 18716209]

Relaix F, Rocancourt D, Mansouri A, Buckingham M. A Pax3/Pax7-dependent population of skeletal muscle progenitor cells. Nature. 2005; 435:948–953. [PubMed: 15843801]

Rowlerson A, Radaelli G, Mascarello F, Veggetti A. Regeneration of skeletal muscle in two teleost fish: Sparus aurata and Brachydanio rerio. Cell Tissue Res. 1997; 289:311–322. [PubMed: 9211834]

Rudnicki MA, Jaenisch R. The MyoD family of transcription factors and skeletal myogenesis. Bioessays. 1995; 17:203–209. [PubMed: 7748174]

Runfola V, Sebastian S, Dilworth FJ, Gabellini D. Rbfox proteins regulate tissue-specific alternative splicing of Mef2D required for muscle differentiation. J Cell Sci. 2015; 128:631–637. [PubMed: 25609712]

Saera-Vila A, Kasprick DS, Junttila TL, Grzegorski SJ, Louie KW, Chiari EF, Kish PE, Kahana A. Myocyte dedifferentiation drives extraocular muscle regeneration in adult zebrafish. Invest Ophthalmol Vis Sci. 2015; 56:4977–4993. [PubMed: 26230763]

Saera-Vila A, Kish PE, Kahana A. Fgf regulates dedifferentiation during skeletal muscle regeneration in adult zebrafish. Cell Signal. 2016; 28:1196–1204. [PubMed: 27267062]

Sambasivan R, Yao R, Kissenpfennig A, Van Wittenberghe L, Paldi A, Gayraud-Morel B, Guenou H, Malissen B, Tajbakhsh S, Galy A. Pax7-expressing satellite cells are indispensable for adult skeletal muscle regeneration. Development. 2011; 138:3647–3656. [PubMed: 21828093]

Schiaffino S, Reggiani C. Fiber types in mammalian skeletal muscles. Physiol Rev. 2011; 91:1447–1531. [PubMed: 22013216]

Seale P, Bjork B, Yang W, Kajimura S, Chin S, Kuang S, Scime A, Devarakonda S, Conroe HM, Erdjument-Bromage H, et al. PRDM16 controls a brown fat/skeletal muscle switch. Nature. 2008; 454:961–967. [PubMed: 18719582]

Seale P, Sabourin LA, Girgis-Gabardo A, Mansouri A, Gruss P, Rudnicki MA. Pax7 is required for the specification of myogenic satellite cells. Cell. 2000; 102:777–786. [PubMed: 11030621]

Seger C, Hargrave M, Wang X, Chai RJ, Elworthy S, Ingham PW. Analysis of Pax7 expressing myogenic cells in zebrafish muscle development, injury, and models of disease. Dev Dyn. 2011; 240:2440–2451. [PubMed: 21954137]

Shefer G, Van de Mark DP, Richardson JB, Yablonka-Reuveni Z. Satellite-cell pool size does matter: Defining the myogenic potency of aging skeletal muscle. Dev Biol. 2006; 294:50–66. [PubMed: 16554047]

Shefer G, Wleklinski-Lee M, Yablonka-Reuveni Z. Skeletal muscle satellite cells can spontaneously enter an alternative mesenchymal pathway. J Cell Sci. 2004; 117:5393–5404. [PubMed: 15466890]

Siegel AL, Gurevich DB, Currie PD. A myogenic precursor cell that could contribute to regeneration in zebrafish and its similarity to the satellite cell. FEBS J. 2013; 280:4074–4088. [PubMed: 23607511]

Sousa S, Afonso N, Bensimon-Brito A, Fonseca M, Simões M, Leon J, Roehl H, Cancela ML, Jacinto A. Differentiated skeletal cells contribute to blastema formation during zebrafish fin regeneration. Development. 2011; 138:3897–3905. [PubMed: 21862555]

Stellabotte F, Dobbs-McAuliffe B, Fernandez DA, Feng X, Devoto SH. Dynamic somite cell rearrangements lead to distinct waves of myotome growth. Development. 2007; 134:1253–1257. [PubMed: 17314134]

Stewart S, Stankunas K. Limited dedifferentiation provides replacement tissue during zebrafish fin regeneration. Dev Biol. 2012; 365:339–349. [PubMed: 22426105]

Talbot JC, Amacher SL. A streamlined CRISPR pipeline to reliably generate zebrafish frameshifting alleles. Zebrafish. 2014; 11:583–585. [PubMed: 25470533]

Talbot J, Maves L. Skeletal muscle fiber type: using insights from muscle developmental biology to dissect targets for susceptibility and resistance to muscle disease. Wiley Interdiscip Rev Dev Biol. 2016; 5:518–534. [PubMed: 27199166]

Tang Q, Moore JC, Ignatius MS, Tenente IM, Hayes MN, Garcia EG, Torres Yordán N, Bourque C, He S, Blackburn JS, Look AT, Houvras Y, Langenau DM. Imaging tumour cell heterogeneity following cell transplantation into optically clear immunedeficient zebrafish. Nat Commun. 2016; 7:10358. [PubMed: 26790525]

Tee JM, Sartori da Silva MA, Rygiel AM, Muncan V, Bink R, van den Brink GR, van Tijn P, Zivkovic D, Kodach LL, Guardavaccaro D, Diks SH, Peppelenbosch MP. asb11 is a regulator of embryonic and adult regenerative myogenesis. Stem Cells Dev. 2012; 21:3091–3103. [PubMed: 22512762]

Trinh le A, Hochgreb T, Graham M, Wu D, Ruf-Zamojski F, Jayasena CS, Saxena A, Hawk R, Gonzalez-Serricchio A, Dixson A, Chow E, Gonzales C, Leung HY, Solomon I, Bronner-Fraser M, Megason SG, Fraser SE. A versatile gene trap to visualize and interrogate the function of the vertebrate proteome. Genes Dev. 2011; 25:2306–2320. [PubMed: 22056673]

Underwood JG, Boutz PL, Dougherty JD, Stoilov P, Black DL. Homologues of the Caenorhabditis elegans Fox-1 protein are neuronal splicing regulators in mammals. Mol Cell Biol. 2005; 25:10005–10016. [PubMed: 16260614]

van Raamsdonk W, Tekronnie G, Pool CW, van de Laarse W. An immune histochemical and enzymic characterization of the muscle fibres in myotomal muscle of the teleost Brachydanio rerio, Hamilton-Buchanan. Acta histochem. 1980; 67:200–216. [PubMed: 6452016]

Venables JP, Lapasset L, Gadea G, Fort P, Klinck R, Irimia M, Vignal E, Thibault P, Prinos P, Chabot B, Abou Elela S, Roux P, Lemaitre JM, Tazi J. MBNL1 and RBFOX2 cooperate to establish a splicing programme involved in pluripotent stem cell differentiation. Nat Commun. 2013; 4:2480. [PubMed: 24048253]

von Maltzahn J, Jones AE, Parks RJ, Rudnicki MA. Pax7 is critical for the normal function of satellite cells in adult skeletal muscle. Proc Natl Acad Sci USA. 2013; 110:16474–16479. [PubMed: 24065826]

Wan J, Ramachandran R, Goldman D. HB-EGF is necessary and sufficient for Müller glia dedifferentiation and retina regeneration. Dev Cell. 2012; 22:334–347. [PubMed: 22340497]

Wang JH, Wang QJ, Wang C, Reinholt B, Grant AL, Gerrard DE, Kuang S. Heterogeneous activation of a slow myosin gene in proliferating myoblasts and differentiated single myofibers. Dev Biol. 2015; 402:72–80. [PubMed: 25794679]

Waterman RE. Development of the lateral musculature in the teleost, Brachydanio rerio: A fine structural study. Am J Anat. 1969; 125:457–493. [PubMed: 5822973]

Wei C, Qiu J, Zhou Y, Hu J, Ouyang K, Banerjee I, Zhang C, Chen B, Li H, Chen J, Song LS, Fu XD. Repression of the Central Splicing Regulator RBFox2 is functionally linked to pressure overload-induced heart failure. Cell Rep. 2015; 10:1521–1533.

Weintraub H, Davis R, Tapscott S, Thayer M, Krause M, Benezra R, Blackwell TK, Turner D, Rupp R, Hollenberg S, et al. The myoD gene family: Nodal point during specification of the muscle cell lineage. Science. 1991; 251:761–766. [PubMed: 1846704]

Weyn-Vanhentenryck SM, Mele A, Yan Q, Sun S, Farny N, Zhang Z, Xue C, Herre M, Silver PA, Zhang MQ, Krainer AR, Darnell RB, Zhang C. HITS-CLIP and integrative modeling define the Rbfox splicing-regulatory network linked to brain development and autism. Cell Rep. 2014; 6:1139–1152. [PubMed: 24613350]

Windner SE, Doris RA, Ferguson CM, Nelson AC, Valentin G, Tan H, Oates AC, Wardle FC, Devoto SH. Tbx6, Mesp-b and Ripply1 regulate the onset of skeletal myogenesis in zebrafish. Development. 2015; 142:1159–1168. [PubMed: 25725067]

Yang G, Huang SC, Wu JY, Benz EJ Jr. Regulated Fox-2 isoform expression mediates protein 4.1R splicing during erythroid differentiation. Blood. 2008; 111:392–401. [PubMed: 17715393]

Yeo GW, Coufal NG, Liang TY, Peng GE, Fu XD, Gage FH. An RNA code for the FOX2 splicing regulator revealed by mapping RNA-protein interactions in stem cells. Nat Struct Mol Biol. 2009; 16:130–137. [PubMed: 19136955]

Yeo GW, Xu X, Liang TY, Muotri AR, Carson CT, Coufal NG, Gage FH. Alternative splicing events identified in human embryonic stem cells and neural progenitors. PLoS Comput Biol. 2007; 3:1951–1967. [PubMed: 17967047]

Zammit PS, Relaix F, Nagata Y, Ruiz AP, Collins CA, Partridge TA, Beauchamp JR. Pax7 and myogenic progression in skeletal muscle satellite cells. J Cell Sci. 2006; 119:1824–1832. [PubMed: 16608873]

Zhang H, Anderson JE. Satellite cell activation and population on single muscle-fiber cultures from adult zebrafish (Danio rerio). J Exp Biol. 2014; 217:1910–1917. [PubMed: 24577448]

Zhu H, Hasman RA, Barron VA, Luo G, Lou H. A nuclear function of Hu proteins as neuron-specific alternative RNA processing regulators. Mol Biol Cell. 2006; 17:5105–5114. [PubMed: 17035636]

HIGHLIGHTS

- Cells similar to mammalian satellite cells are present in adult zebrafish skeletal muscle.
- Adult Pax7-positive satellite-like cells proliferate and contribute to skeletal muscle repair after injury.
- RNA-binding proteins Rbfox2 and Rbfox1l are expressed in satellite cells and regenerating myofibers, respectively, during skeletal muscle repair.
- Pax7 is required for skeletal muscle repair in adult zebrafish.

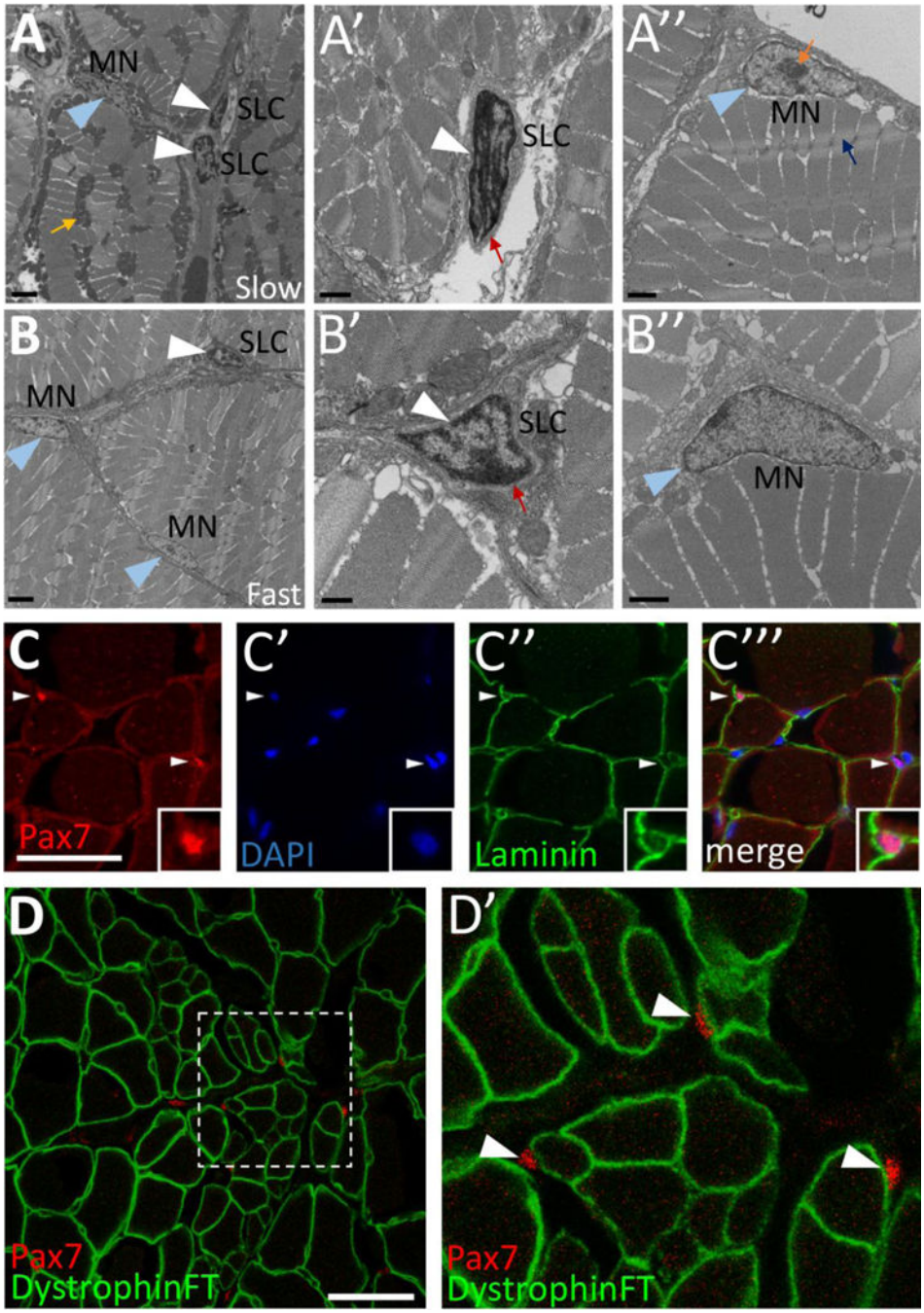

Figure 1. Cells with satellite cell features are present in adult zebrafish skeletal muscle

(A–B) Transmission electron microscopy (TEM) on adult zebrafish tail skeletal muscle from slow-twitch (A–A″) and fast-twitch (B–B″) muscle fiber domains. (A) TEM of slow muscle reveals mitochondrial-rich muscle fibers (mustard arrow points to a cluster of dark gray mitochondria), putative satellite-like cells (SLCs; white arrowheads), and myonuclei (MN; blue arrowhead points to a myonucleus). (A′) Higher magnification view of a SLC containing dense heterochromatin (white arrowhead) and surrounded by basal lamina (red arrow). (A″) A myonucleus (MN; blue arrowhead) located within the muscle fiber

membrane. Myonuclei are characterized by a lack of dense heterochromatin and often by a prominent nucleolus (orange arrow). An adjacent myofibril is indicated by a blue arrow. (B) TEM of fast muscle reveals fewer mitochondria, a putative SLC (white arrowhead), as well as myonuclei (MN, blue arrowheads). (B′) Higher magnification view of a SLC containing dense heterochromatin (white arrowhead) and surrounded by basal lamina (red arrow). (B″) A myonucleus (MN; blue arrowhead) located within the muscle fiber membrane shows similar characteristics to slow muscle myonuclei. (CC′″) Pax7-positive cells (red; white arrowheads) are localized within the basal lamina of adult zebrafish skeletal muscle (anti-Laminin in green) (inset shows enlarged view of Pax7-positive cell). DAPI labeling confirms Pax7 localization in nuclei. (D–D′) Pax7-positive cells (red; arrowheads) are located outside of the muscle fiber membrane, marked by a Dystrophin FlipTrap transgenic line. (D′) Magnified view of boxed region in D. Scale bar in A, B is 2 μm, in A′, A″, B″ is 1 μm, in B′ is 500 nm, and in C and D is 30 μm.

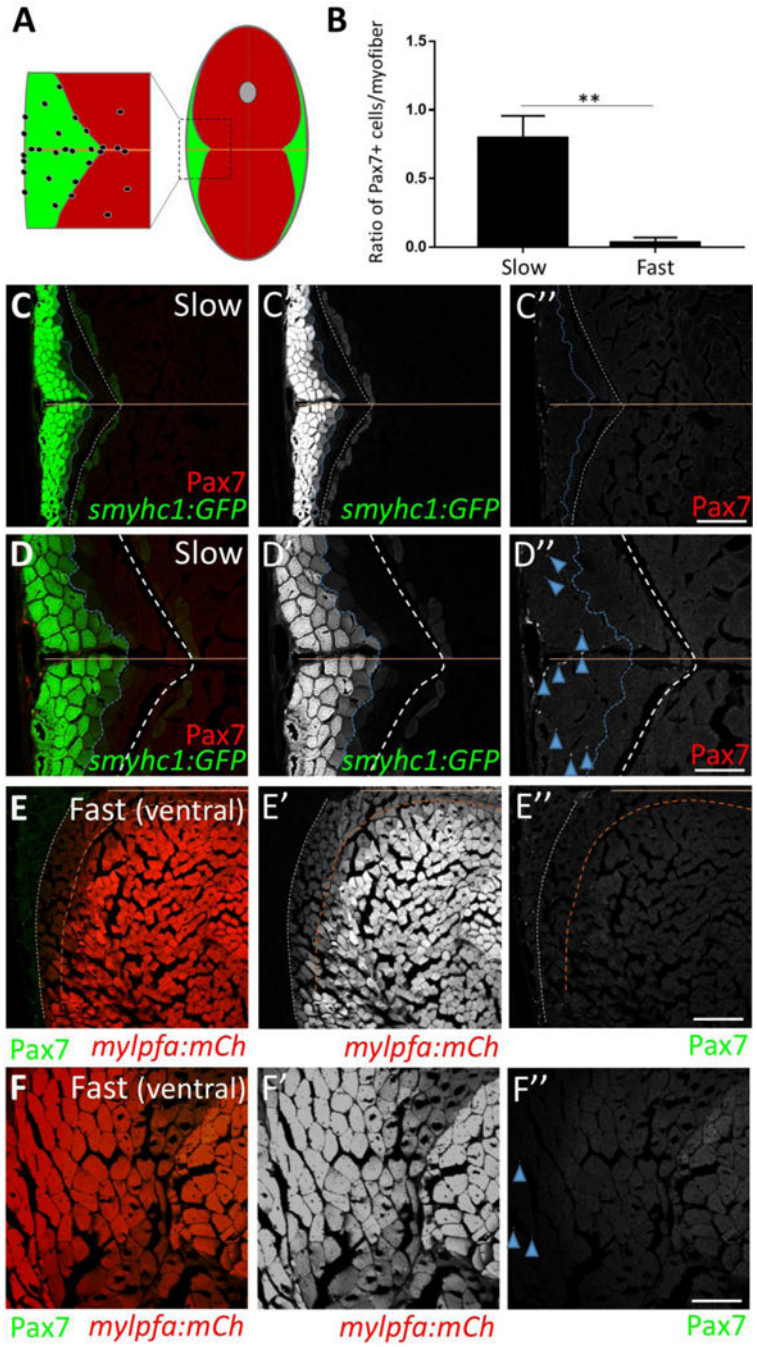

Figure 2. Adult zebrafish satellite-like cells are concentrated predominantly in slow muscle

(A) Schematic of cross-section through adult zebrafish trunk musculature, depicting fast-twitch (red) and slow-twitch (green) muscle fiber domains and a concentration of SLCs (black dots) within the slow muscle domain. The horizontal myoseptum is indicated by a brown line; the gray circle at the dorsal midline depicts the spinal cord. (B) The number of Pax7-positive cells, normalized to total myofiber number, is significantly higher in slow versus fast muscle; Student's t-test (p**<0.01). (C–C″) Pax7-positive cells (in red) are more common within slow muscle. Slow muscle fibers are marked with *smyhc1*-driven GFP (left

of the dotted blue line). The boundary between slow and fast muscle fiber domains is marked by a dotted white line. The area between dotted blue and dotted white lines may represent muscle fibers with an intermediate identity. The horizontal myoseptum is indicated by a brown line. (D–D″) Higher magnification view of slow muscle. For quantification shown in B, Pax7-positive cells (D″; examples depicted by blue arrowheads) within the *smyhc1:GFP*-positive domain (left of the dotted blue line) were counted and normalized to the number of *smyhc1:GFP*-positive myofibers in the same area. (E–E″) Pax7-positive cells (in green) are rare within ventral fast muscle. Fast (ventral) muscle fibers are marked with *mylpfa*-driven mCherry (right of the dotted brown line). The area between dotted brown and white lines (weakly expressing *mylpfa:mCherry*) may represent intermediate muscle fiber identity. A dotted white line separates fast and slow muscle domains. (F–F″) Higher magnification image of fast muscle. For quantification shown in B, Pax7-positive cells (F″; blue arrowheads) within the *mylpfa:mCherry*-positive domain were counted and normalized to the number of *mylpfa:mCherry*-positive myofibers in the same area. Scale bar in C” and E” is 150 μm and in D” and F” is 75 μm.

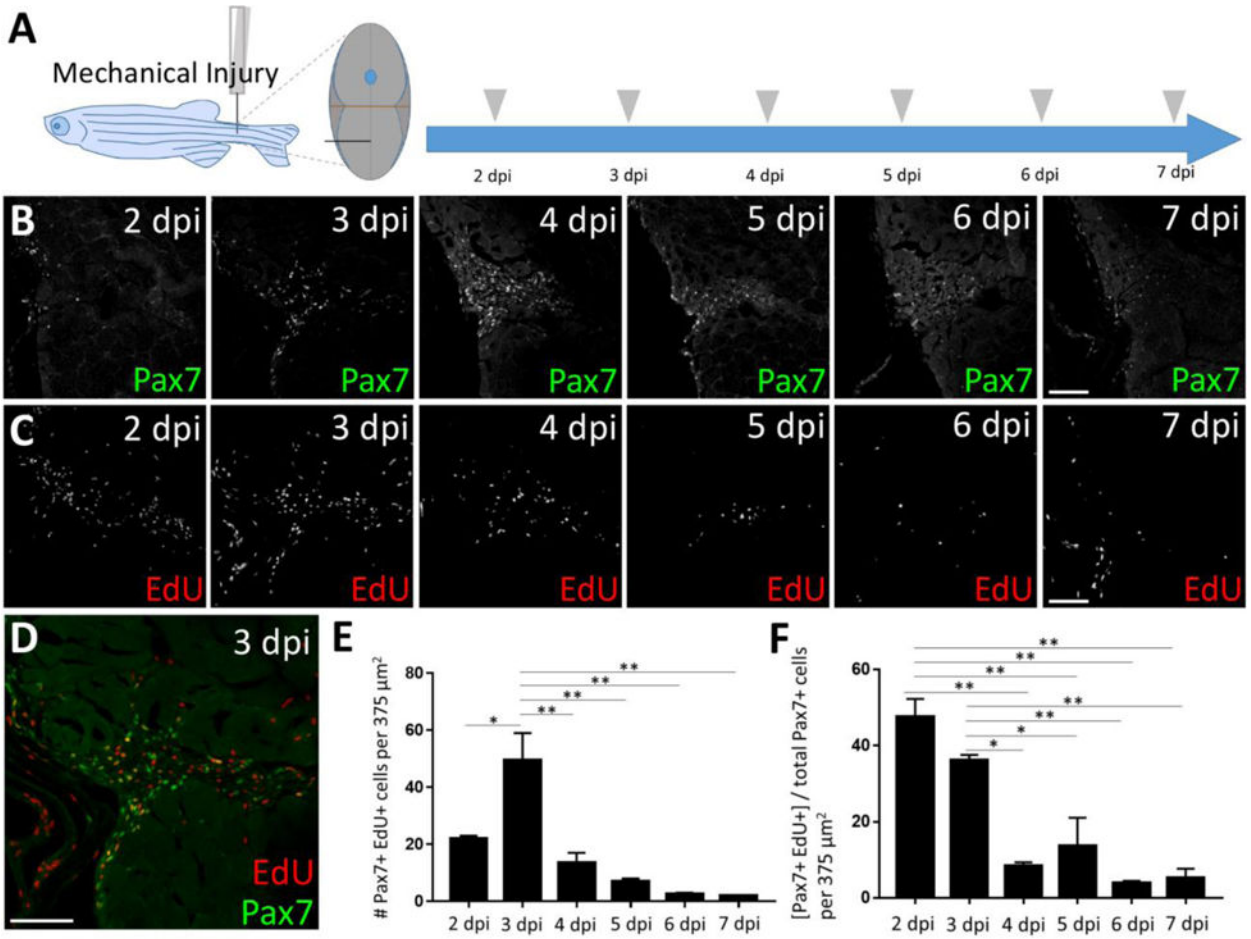

Figure 3. Satellite-like cells in adult zebrafish skeletal muscle proliferate after mechanical injury

(A) Schematic of experimental procedure, in which mechanical injury is performed by a single needle-stick into tail skeletal muscle. The approximate position of needle-stick injury in the ventral myotome is indicated in cross-sectional view. EdU was administered (gray arrowhead) by intraperitoneal injection at each post-injury time-point, allowing for EdU incorporation into S-phase cells, and fish were sacrificed 4 hours later (acute EdU labeling). Tissue was collected at 2, 3, 4, 5, 6, and 7 dpi. (B) Pax7-positive cell numbers increase at the injury site and peak at 4 days post-injury (dpi). (C) Acute EdU labeling indicates robust proliferation at the injury site at 2 and 3 dpi that declines thereafter. (D) Overlap of Pax7 and EdU at 3 dpi indicates satellite-like cell proliferation post-injury. (E) Quantification of Pax7 and EdU double positive cells at each post-injury time-point reveals a peak number of proliferating satellite-like cells at 3 dpi in an 375 μm^2 area encompassing the injury site; p*<0.05; p**<0.01. (F) Quantification of the percentage of Pax7-positive cells that are EdU-positive (out of total Pax7-positive cell population) at each post-injury time-point indicates that nearly 50% of Pax7-positive cells are proliferating at 2 dpi, and ~35% are proliferating at 3 dpi. The percentage of Pax7-positive cells that are EdU-positive at later post-injury time-points (4–7 dpi) is significantly less; p*<0.05; p**<0.01. One-way ANOVA followed by Tukey's multiple comparisons test was performed for statistical analyses. Scale bar in all panels is 75 µm.

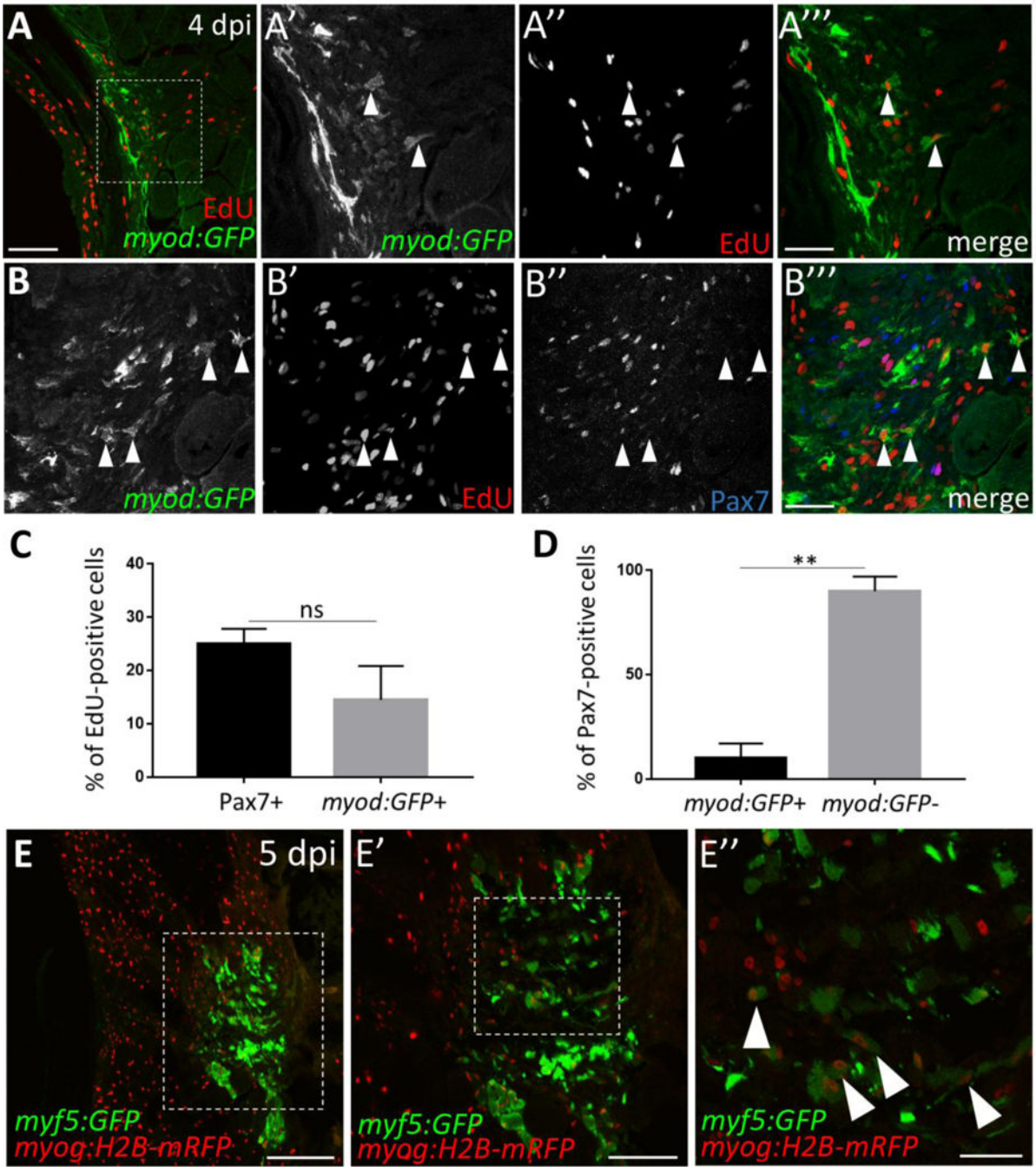

Figure 4. Myoblast-like cells, detected using *myf5:GFP* and *myod:GFP* transgene expression, are present post-injury in adult zebrafish skeletal muscle

(A) The *myod:GFP* transgenic line identifies myoblast-like cells at 4 dpi. (A′–A′″) Magnified view of boxed area in A, showing *myod:GFP* expression (A′), EdU incorporation after an acute EdU pulse (A”), and the overlay (A′″) at 4 dpi. Double-positive cells are indicated by arrowheads. (B–B′″) At 4 dpi, *myod:GFP*-expressing cells are largely Pax7-negative (examples indicated by arrowheads). (C) Percentage of total proliferating cells (i.e. those that incorporate EdU) at 4 dpi that are Pax7-positive (25%) versus *myod:GFP*-positive (15%). The percentage of proliferating cells that are Pax7-positive (25%) is similar to that

shown in Fig. S3I and is slightly higher than the percentage of proliferating cells that are *myod:GFP*-positive (15%), although the difference is not statistically significant. (D) Percentage of Pax7-expressing cells at 4 dpi that are *myod:GFP*-positive (10%) versus *myod:GFP*-negative (90%), p**<0.01. (E) *myf5:GFP*-positive cells are present at the injury site at 5 dpi. (E′) Magnified view of boxed region in E. (E”) Magnified view of boxed region in E′ reveals *myf5:GFP*-positive cells that are *myog:H2B-mRFP*-positive (arrowheads). Scale bar in A and E′ is 75 μm, in E is 150 μm, and in A′–B′″ and E” is 30 μm.

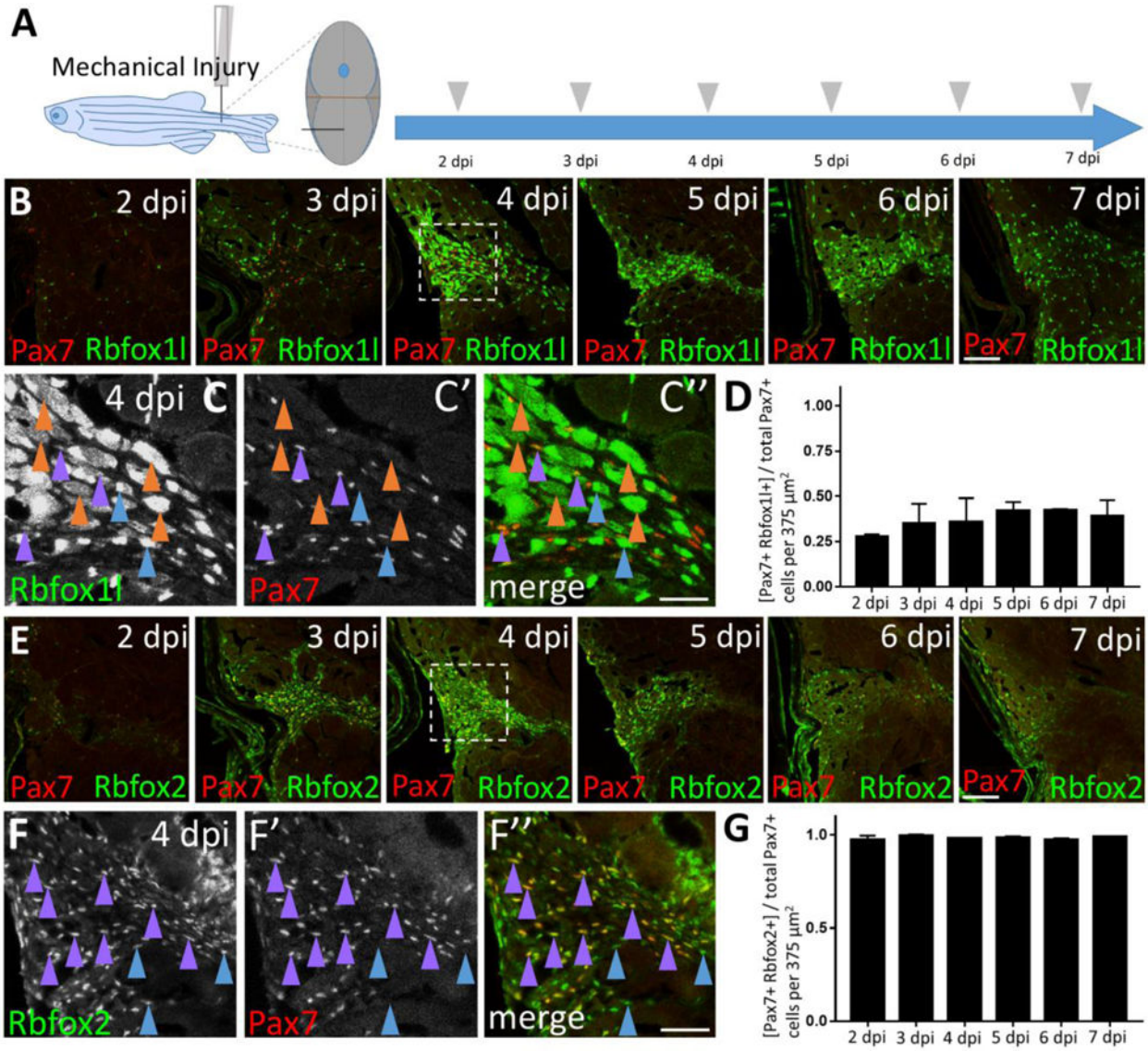

Figure 5. Satellite-like cells express Rbfox1l and Rbfox2 RNA-binding proteins after mechanical injury of adult zebrafish skeletal muscle

(A) Schematic of experimental procedure, which is identical to that described Fig. 3A. (B) Rbfox1l (green) is robustly expressed beginning at 4 dpi, coinciding with the onset of new myofiber formation. Pax7 expression (overlaid in red) is the same as shown in Fig. 3C; the merge here shows overlap of Pax7 and Rbfox1l expression. The boxed region at 4 dpi is magnified in C–C”. (C–C”) Magnified view of boxed area in B, showing expression of Rbfox1l (C) and Pax7 (C′), and the overlay (C”) at 4 dpi. Examples of Pax7-positive, Rbfox1l-positive cells are indicated by purple arrowheads and of Pax7-negative, Rbfox1l-positive cells by blue arrowheads. Rbfox1l expression is observed in the cytoplasm of presumptive newly-forming myofibers (orange arrowheads indicate examples). Rbfox1l expression in uninjured areas surrounding the injury site appears less uniform in muscle fiber nuclei (compared to Fig. S6 D–D″) as laser intensity was reduced to prevent over-saturation of signals within the injury site. (D) Ratio of Pax7-positive cells that are Rbfox1l-

positive at post-injury time-points 2–7 dpi. (E) Onset of Rbfox2 expression (green) at 3 dpi is earlier than Rbfox1l, and closely resembles post-injury Pax7 expression (overlaid in red). The sections are alternating with those in B. The boxed region at 4 dpi is magnified in F–F". (F–F") Magnified view of boxed area in C, showing expression of Rbfox2 (F) and Pax7 (F′), and the overlay (F") at 4 dpi. Examples of Pax7-positive, Rbfox2-positive cells are indicated by purple arrowheads, and of Pax7-negative, Rbfox2-positive cells by blue arrowheads. (G) Ratio of Pax7-positive cells that are Rbfox2-positive at post-injury time-points 2–7 dpi. Scale bar in B and E is 75 μm, and in C–C" and F–F" is 30 μm.

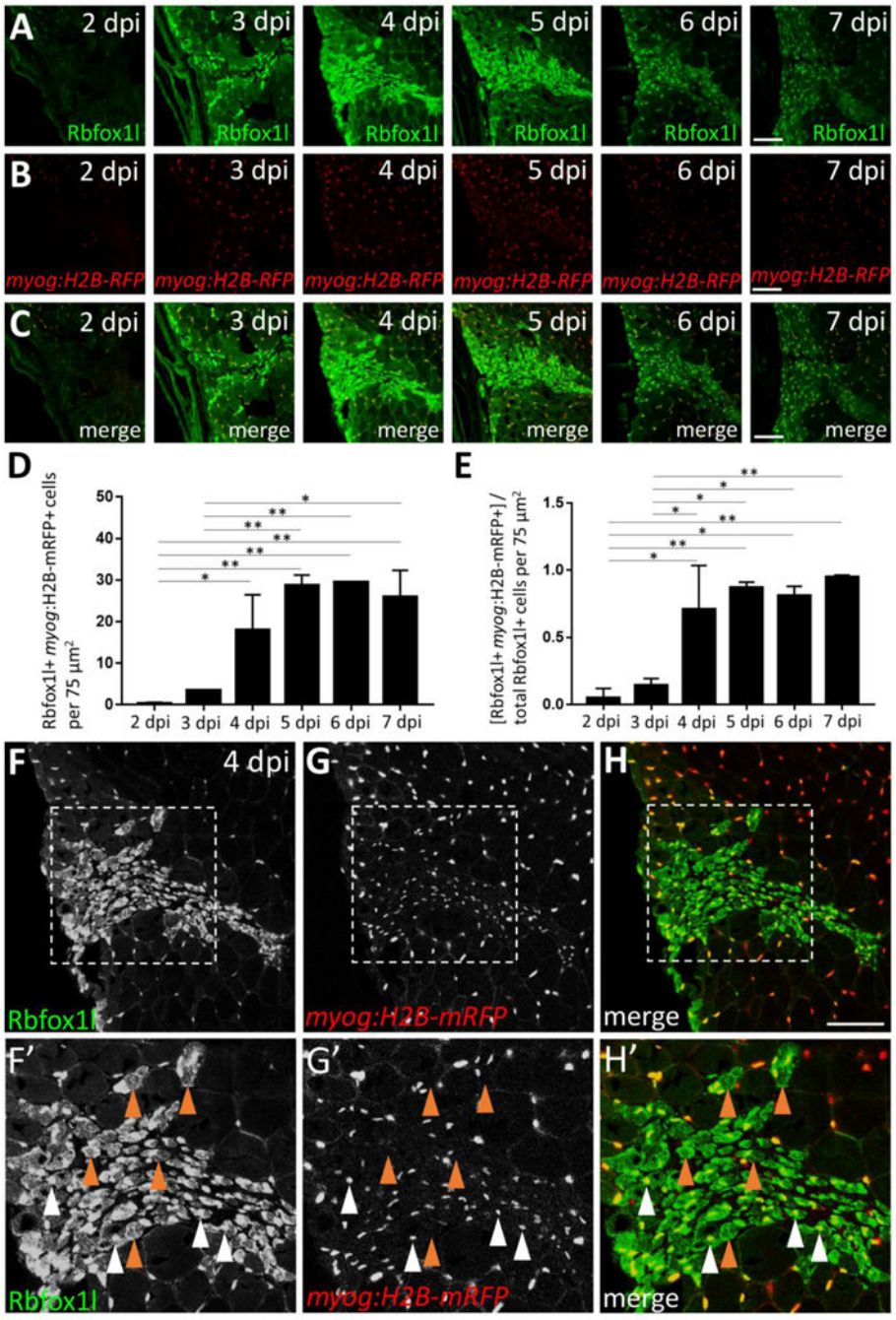

Figure 6. Rbfox1l is expressed predominantly in the nucleus and cytoplasm of newly-forming myofibers during skeletal muscle repair

(A) Injury time-course experiment performed in the *myog:H2B-mRFP* transgenic line showing Rbfox1l expression at each post-injury time-point. (B) *myog:H2B-mRFP* expression is readily observed within the injury site by 4 dpi. (C) Overlay of Rbfox1l and *myog:H2B-mRFP* expression. (D) Total number of Rbfox1l, *myog:H2B-mRFP* double-positive cells at 2–7 dpi in a 75 μm^2 area within the injury site (to exclude Rbfox1l-positive; *myog:H2B-mRFP*-positive myonuclei within surrounding uninjured fibers). (E) Ratio of Rbfox1l-positive cells that are *myog:H2B-mRFP*-positive at 2–7 dpi. One-way ANOVA

followed by Tukey's multiple comparisons test was performed for statistical analyses in D and E ($p^{*}<0.05$; $p^{**}<0.01$). (F–H) Higher magnification view of 4 dpi injury site shown in A–C. (F′–H′) Area shown is the boxed region in F–H. A majority of Rbfox1l-positive nuclei are also positive for *myog:H2B-mRFP* (examples indicated by white arrowheads), as expected from the large overlap of these two markers in differentiated muscle outside of the injury site. Rbfox1l expression in uninjured areas surrounding the injury site appears less uniform in muscle fiber nuclei in this figure (compared to Fig. S6 D–D″) as laser intensity was reduced to prevent over-saturation of signals within the injury site. Some newly-forming myofibers that express Rbfox1l in the nucleus and/or cytoplasm are *myog:H2B-mRFP*-negative (examples indicated by brown arrowheads). Scale bar in all panels is 75 μm.

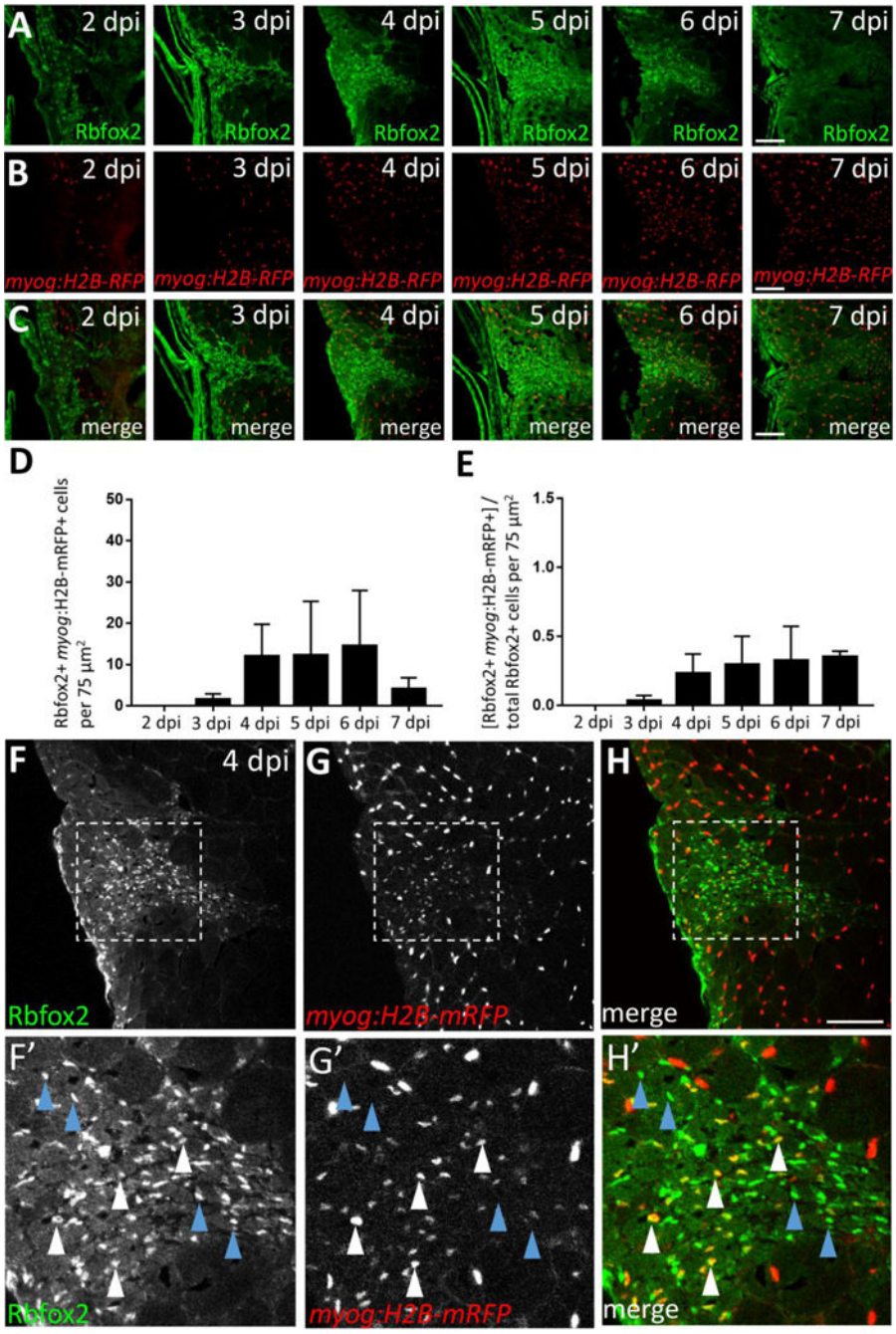

Figure 7. A subset of Rbfox2-expressing cells are *myog:H2B-mRFP*-positive during skeletal muscle repair

(A) Injury time-course experiment performed in *myog:H2B-mRFP* transgenic line showing Rbfox2 expression (on alternating sections with those described in Fig. 6). (B) As shown in Fig. 6B, *myog:H2B-mRFP* expression is readily observed within the injury site by 4 dpi. (C) Overlay of Rbfox2 and *myog:H2B-mRFP* expression. (D) Total number of Rbfox2, *myog:H2B-mRFP* double-positive cells at 2–7 dpi. (E) Ratio of Rbfox2-positive cells that are *myog:H2B-mRFP*-positive at 2–7 dpi. One-way ANOVA followed by Tukey's multiple comparisons test was performed for all of the above statistical analyses; differences among

time-points are not statistically significant. (F–H) Higher magnification view of 4 dpi injury site shown in A–C. (F′–H′) Area shown is the boxed region in F–H that highlights examples of Rbfox2-expressing cells that are *myog:H2B-mRFP*-positive (white arrowheads) and *myog:H2B-mRFP*-negative (blue arrowheads). Scale bar in all panels is 75 μm.

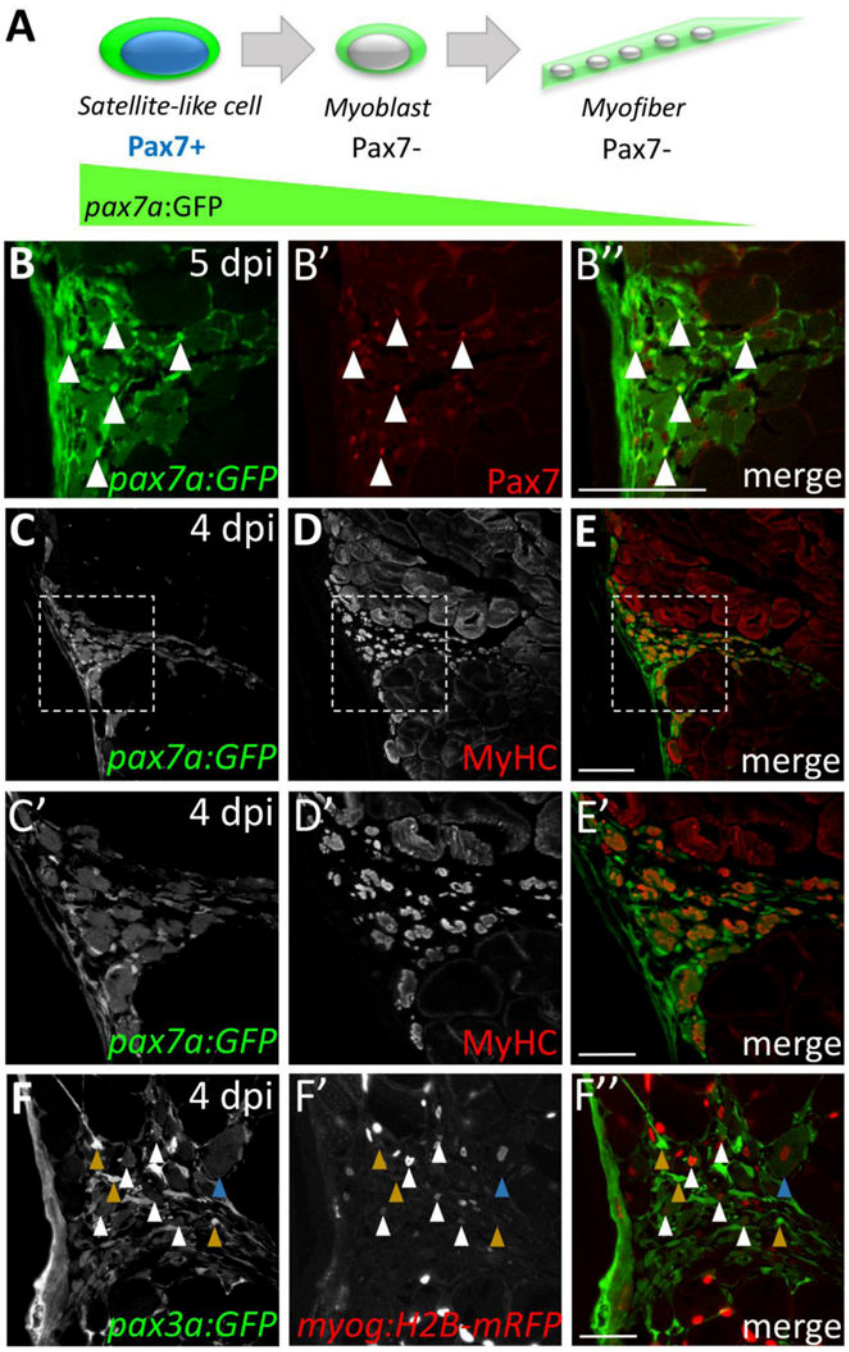

Figure 8. GFP perdurance in the *pax7a:GFP* transgenic line implicates satellite-like cells as a source of new muscle fibers during injury-induced repair

(A) Schematic diagram depicting Pax7 protein and *pax7a:GFP* transgene expression in satellite-like cells and myofibers. *pax7a:GFP*-positive; Pax7-positive cells represent satellite-like cells. Cells that show *pax7a:GFP* expression within the cytoplasm but are Pax7-negative are likely differentiating or differentiated cells in which *pax7a*-driven GFP perdures. (B–B″) At 5 dpi, *pax7a:GFP* and Pax7 double-positive satellite-like cells are present at the injury site (arrowheads); however, GFP expression is also detected in Pax7-negative presumptive newly-forming myofibers. (C–E) At 4 dpi, many cells expressing MyHC (A4.1025), a

differentiation marker, also express *pax7a:GFP*. (C′–E′) Magnified view of boxed region in C–E highlights the overlap of *pax7a:GFP* and MyHC expression. (F–F″) *pax3a:GFP* and *myog:H2B-mRFP* transgene expression overlap in presumptive newly-forming myofibers at 4 dpi (white arrowheads), but *pax3a:GFP*-positive, *myog:H2B-mRFP*-negative are also present (mustard arrowheads). A rare presumptive newly-forming myofiber with a centrally-located nucleus is indicated by a blue arrowhead. Scale bar in B–E is 75 μm, in C′, D′, E′ and F–F" is 30 μm.

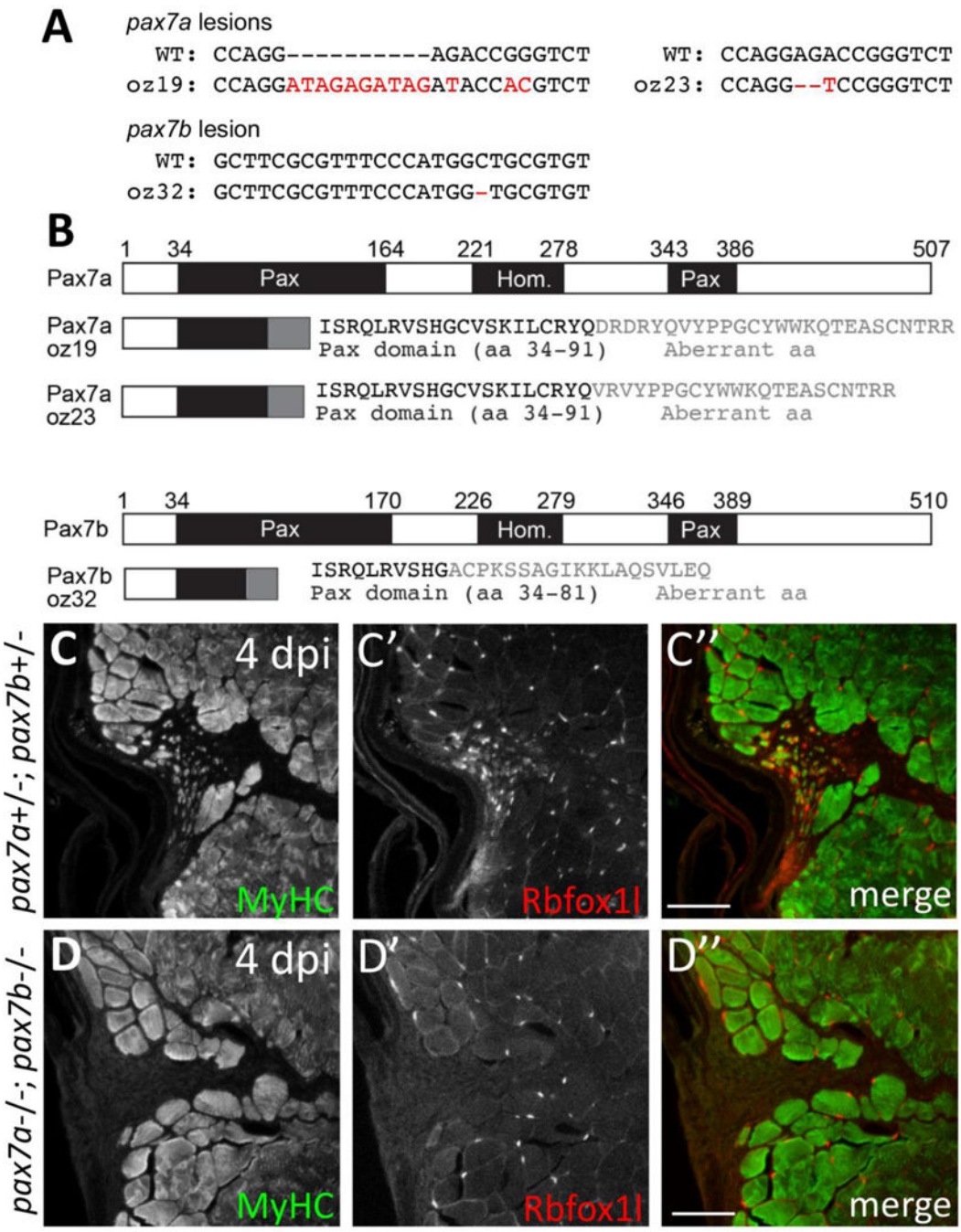

Figure 9. Pax7 function is required for skeletal muscle repair in adult zebrafish

(A) DNA lesions for *pax7a* alleles (*oz19*, *oz23*) and the *pax7b* (*oz32*) allele. Mutant allele sequence is shown below the wild-type sequence. Red letters and dashes indicate the lesion as well as single nucleotide changes near the CRISPR-induced frameshifting mutation. (B) CRISPR-induced frameshifting mutations in exon 2 of *pax7a* and *pax7b* cause truncations in Pax7a and Pax7b proteins, respectively, that eliminate much of the first conserved paired domain (Pax) and the entire homeodomain (Hom) and second Pax domain. The $pax7a^{oz19}$ and $pax7a^{oz23}$ alleles encode the first 91 of 507 amino acids of the Pax7a protein, as well as

an additional 26 and 22 aberrant amino acids, respectively. The *pax7b*^{oz32} allele encodes the first 81 of 510 amino acids of the Pax7b protein, as well as an additional 19 aberrant amino acids. (C–C”) *pax7a+/−*; *pax7b+/−* doubly heterozygous sibling controls show normal muscle repair at 4 dpi, indicated by expression of newly-forming myofiber markers, MyHC (A4.1025) and Rbfox1l. (D–D”) In contrast, *pax7a−/−*; *pax7b−/−* double homozygous mutants are severely deficient in newly-forming myofibers at 4 dpi, indicated by the near absence of MyHC (A4.1025) and Rbfox1l expression within the injury site. The *pax7a*^{oz23} and *pax7b*^{oz32} alleles were used in these experiments. Scale bar in all panels is 75 μm.

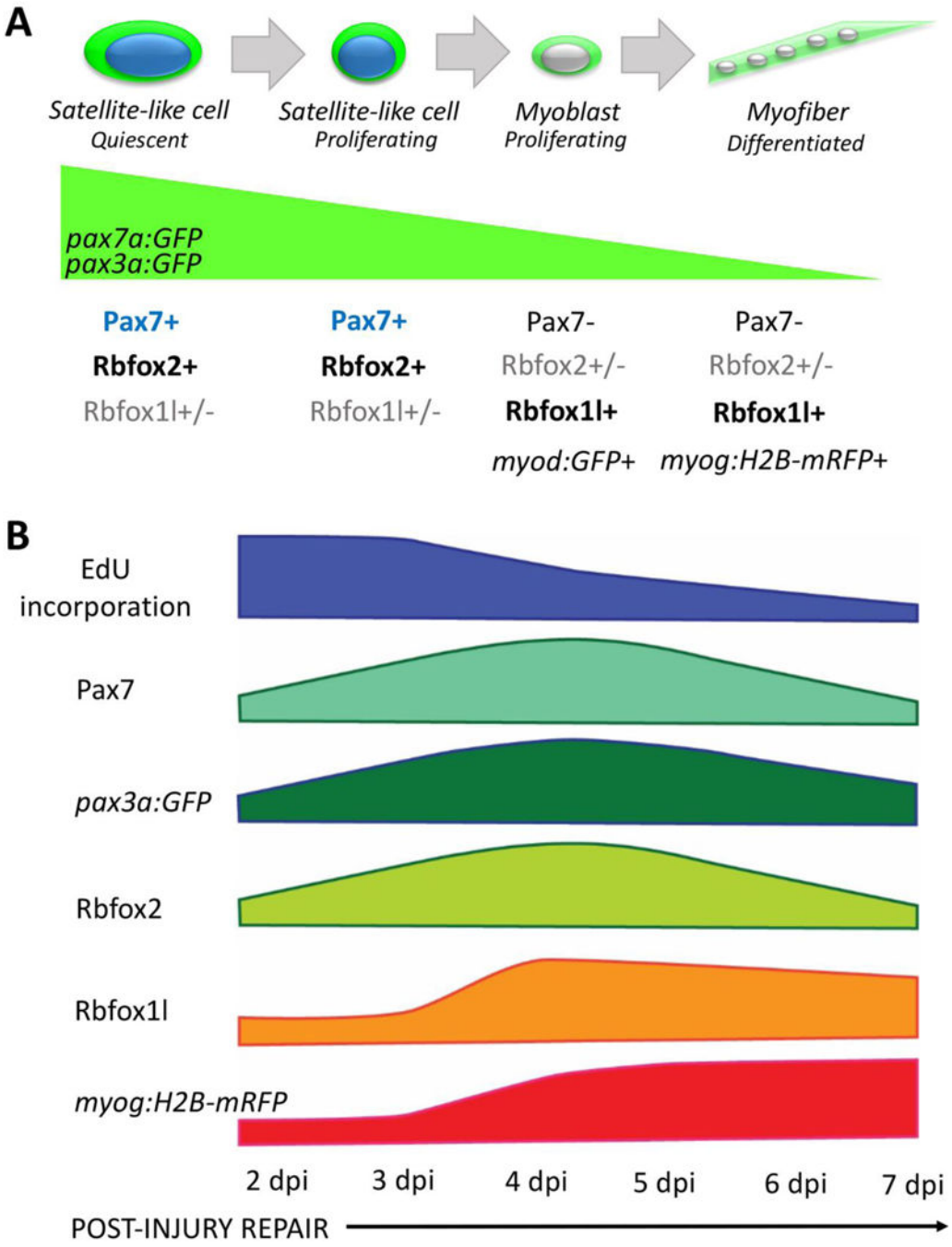

Figure 10. Model depicting changes in gene expression as satellite-like cells differentiate into new muscle fibers during adult zebrafish skeletal muscle repair

(A) Adult zebrafish satellite-like cells express Pax7 and Rbfox2, and in transgenic *pax7a:GFP* and *pax3a:GFP* adults, express GFP. A subset (~37%) express Rbfox1l. During injury-induced repair, some Pax7-expressing satellite cells-like become activated; initially, activated cells proliferate, then down-regulate Pax7 and activate differentiation markers. Although Pax7 protein is largely absent in myoblasts, *pax7a*-driven and *pax3a*-driven GFP perdures in *pax7a:GFP* and *pax3a:GFP* transgenic lines (green wedge). As cells adopt more differentiated fates, Rbfox1l becomes prominently expressed, as do transgenic markers of

myoblasts (*myod:GFP*) and myofibers (*myog:H2B-mRFP*). (B) Diagram depicting marker expression and proliferation status at the population level at the injury site at 2–7 dpi. A large number of proliferating (EdU+) cells are present at the injury site at 2 and 3 dpi, some of which are Pax7-positive. This early proliferation of Pax7-positive satellite-like cells appears to lead to an increase in Pax7-positive cell numbers by 4 dpi. *pax3a:GFP* shows a similar wave of expression that peaks at the time when Pax7-positive cell numbers are highest; however, *pax3a:GFP* expression is also observed at later post-injury time-points (as is *pax7a:GFP* expression). Rbfox2 expression largely mirrors that of Pax7, although Rbfox2 is expressed in some myonuclei of new myofibers that no longer express Pax7. Rbfox1l is robustly expressed at the onset of new myofiber formation (3–4 dpi), with peak expression at 4 dpi in both nucleus and cytoplasm of newly-forming fibers. The number of *myog:H2B-mRFP*-positive cells gradually increase post-injury as myogenic differentiation and new myofiber formation progresses.